

Recent Progress on Textile-Based Triboelectric Nanogenerators

Watcharapong Paosangthong^{a,*}, Russel Torah^a, Steve Beeby^a

^a*School of Electronics and Computer Science, University of Southampton, Southampton, SO171BJ, UK*

**Corresponding author*

E-mail addresses: wp1y15@soton.ac.uk (W. Paosangthong), rnt@ecs.soton.ac.uk (R. Torah), spb@ecs.soton.ac.uk (S. Beeby)

Abstract

Triboelectric nanogenerators (TENG) are one of the most promising candidates for powering wearable and portable devices. Example TENGs have demonstrated flexibility, light weight, biocompatibility, versatility and good performance. Textiles are a potential substrate onto, or into, which wearable technology is increasingly being incorporated but supplying power remains an enduring challenge. TENGs are a potential textile based mechanical energy harvesting power supply and there has been an increasing effort to combine TENGs with fabrics. A significant challenge exists in the integration without losing the performance of the TENG or the original properties (appearance, breathability, washability, and durability) and feel of the textile. Various approaches towards the realisation of textile-based TENGs (T-TENGs) have been demonstrated. Depending on its structure, T-TENGs can be divided into two main types, fabric-based TENG and fibre-based TENG. The fabric-based TENG is composed of conventional and/or modified fabrics, which serve as a substrate and/or a triboelectric material. The fibre-based TENG is fabricated as a single fibre or a collection of interlaced fibres. This paper provides an up to date review of the progress in the research of T-TENGs. The paper covers the basic operating principles, possible operation modes, textile manufacturing methods, material selections, T-TENG fabrication process, surface modification and structural designs. Issues, such as standardised measurement parameters, the challenges and limitations of T-TENG are discussed.

KEYWORDS: Triboelectric nanogenerator, Textile, Fabric, Fiber

1. Introduction

Thanks to the substantial progress in e-textile development, electronic components, such as power storage systems, power management systems, wireless communication systems and transducers, can be embedded in textiles in the form of fibres, yarns and/or fabrics using cost-effective and well-established textile fabrication processes. The rapid growth in the wearable and portable devices market in recent decades has attracted a substantial amount of interest in micro- and nanoenergy research to solve the problem of powering these systems. Since such devices are typically battery powered, they normally operate on an economical energy budget and the recharging/replacement of the batteries is inevitable. The reliance on a battery power supply hinders the realisation of truly integrated wearable electronic systems. An effective solution investigated by many researchers is the implementation of a self-powered system utilising energy harvesting to convert energy from the surrounding environment, such as light, thermal and kinetic energy into electrical energy. The human body is an effective power source for wearable electronics. Activities of daily living, such as footstep or arm movement of a 68-kg adult can deliver approximately 67 W and 60 W of kinetic power, respectively [1]. A small portion of this power will be sufficient to drive many kinds of portable devices. Photovoltaic textiles [2–4], textile-based thermoelectric [5–7] and piezoelectric generators [8–10] have been proposed as wearable harvesters. However, they are not robust and often impractical in real applications. For instance, piezoelectric generators rely on strain, whereas textiles are conformal materials, therefore strain transferred to the load is minimal and thus their power outputs are low.

An alternative transduction technique for converting kinetic energy into electrical energy was proposed by Z. L. Wang's research group in 2012. They demonstrated a flexible triboelectric nanogenerator (TENG) based on the contact electrification and electrostatic induction effect [11]. Subsequently, TENGs have been intensively investigated and developed

both in their performance and applications. A TENG can be used to harvest energy on a large-scale, such as harvesting energy from wind [12–14] or water waves [15,16] or on a small-scale, such as from human motion [17–19]. This approach is well suited to textiles and provides a potentially more efficient way to scavenge the energy from human motion because it relies on relative motion, compressive forces or stretching rather than coupling strain to an active material as in the case of piezoelectric generators. The first textile-based TENGs (T-TENGs) was introduced by Zhong et al. in 2014 [20]. It comprised two modified cotton yarns twisted together, which can convert biomechanical motions/vibration energy into electricity and power mobile medical systems. Other examples of first generation T-TENGs include the research of Jung et al. [21], Zhou et al. [22] and Pu et al. [23]. T-TENGs have been produced in the form of fibres, threads and fabrics, which provide a convenient approach for their integration with wearable e-textile electronics. In addition to harvesting energy from the human body via clothing, there is a possibility to utilise T-TENGs in many other applications. Textiles are found in many areas, including home interiors (carpeting, bedding, furnishing), leisure (bags, backpacks, tents, nets, flags), transportation (car/train interiors), engineering (ground reinforcement and marine textiles) and medicine (bandages and medical implants). As examples, a bedding and flag-type T-TENG were demonstrated by Lin et al. and Zhao et al., respectively [24,25].

This article reviews the recent development and novel technique applied in T-TENGs. Whereas most review papers broadly describe flexible TENGs, this paper will focus on textile applications only. Firstly, the operating modes of T-TENG and their working principles are described. Next, basic textile manufacturing methods are introduced since this influences the choice of materials and assembly methods for T-TENGs. The surface modification used to enhance the performance of T-TENG is described and examples of various types of T-TENG categorised according to their structural and material design are covered in detail. Finally, their

performance, measurement of performance and the practicalities in real applications scenarios of T-TENGs are summarised.

2. Fundamental operation modes

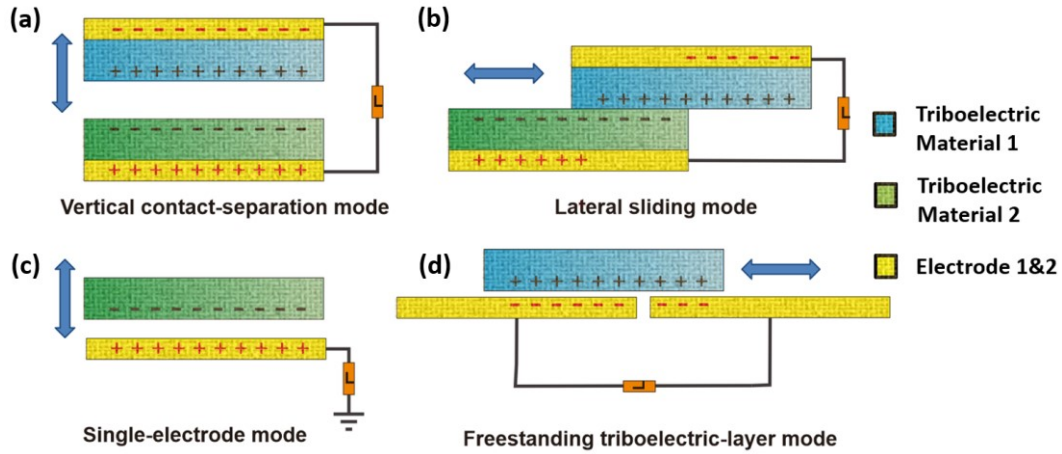


Fig. 1 Four fundamental operation modes of TENG: **a)** Vertical contact-separation mode (CS-mode), **b)** lateral sliding mode (LS-mode), **c)** single-electrode mode (SE-mode) and **d)** freestanding triboelectric-layer mode (FT-mode)

TENGs can be used to transform kinetic energy occurring during frictional contact between two materials with different electron affinities into electricity based on the triboelectric effect and electrostatic induction, which are coupled together [26]. The triboelectric effect is a type of contact electrification, in which electrical charges are separated and transferred from one material to the other material when they are brought into a frictional contact. The surface of the material with the higher electron affinity will become negatively charged, while the other surface will become positively charged. The external kinetic energy will periodically drive the charged surfaces resulting in a relative displacement between the surfaces and electrodes and thus leading to a periodic change in an induced potential difference between the electrodes. When the electrodes are connected through an electrical load, free electrons will continuously flow back and forth between the electrodes to reduce the induced potential difference and to maintain the electrostatic equilibrium between them. With this principle, an AC power output is extracted at the load. Depending on different configurations of the triboelectric materials and

the electrodes, and their relative movement, the fundamental operation modes of TENG can be categorised into the four following modes [27,28].

2.1. Vertical contact-separation mode (CS-mode)

As shown in Fig. 1(a), a TENG operating in the CS-mode consists normally of two dissimilar triboelectric materials facing to each other with an electrode deposited on the reverse side forming a stacked configuration. To be able to contain the charge on the surface, at least one of the triboelectric materials has to be a dielectric. A frictional contact between the triboelectric materials will lead to a charge transfer and thus two oppositely charged surfaces. As the two materials are separated, the potential difference between the two electrodes increases. The electric potential of the electrode deposited close to the positive surface is higher than that of the electrode deposited close to the negative surface. To balance the potential, the electrons flow from the electrode with lower potential to the one with higher potential until the potential difference disappears. When the gap is reduced, the potential difference is built up again because the number of the electrons in the electrode exceeds the surface charges and thus these excess electrons have to flow back.

Most examples of T-TENGs are operated in this mode because of the nature of human movement and the simplicity of the fabrication. For example, they can be built inside shoe insoles to harvest energy from human walking [29] or embedded inside a fabric to generate power from pressing or stretching the fabric. Such motions lead to a contact-separation movement between the triboelectric materials. The structure of this type of TENG has been designed in various forms, such as multi-stacked fabrics [30–35] or yarns [20,36–42].

2.2. Lateral sliding mode (LS-mode)

The operation of the LS-mode is shown in Fig. 1(b). Similar to the contact mode, it comprises two triboelectric materials with two back electrodes. When the top and the bottom triboelectric materials are fully aligned, the positive and negative surface charges are

compensated, thus there is no potential difference between the electrodes. In contrast, when the materials are misaligned, there is a potential building up in the non-overlapping parts of the electrodes and a resultant potential difference occurs. As a result, electrons flow between the electrodes. Once the substrates move back to the initial aligned position, the electrons have to flow back to balance the potential. The AC output is obtained from the periodic sliding between the materials [26]. Compared to the CS-mode, the in-plane movements enable a TENG to harvest energy from planar motion [43], disc rotations [44] or cylindrical rotations [45]. Additionally, a larger frictional contact occurring during sliding enhances the charge separation and thus improves the performance of TENG. However, the higher friction can lead to greater material abrasion and, due to the lateral movement of the assembly, at least twice as much area is required as the CS-mode equivalent.

To improve the performance of this mode, most T-TENGs are fabricated with a linear-grating structure [21], since this reduces the required sliding distance to operate the device with the same surface area and such a design dramatically increases the frequency and the amplitude of the short-circuit current (I_{SC}) proportional to the size and the number of grating strips. However, the open-circuit voltage (V_{OC}) drops due to a growth in the capacitance of the electrodes [46]. An early example of the LS-mode T-TENGs was demonstrated by Jung et al. in 2014 [21]. They fabricated a grated TENG comprising alternating strips of polyimide (PI) and polyurethane (PU) mounted on a sleeve and alternating strips of polydimethylsiloxane (PDMS) and aluminium (Al) attached to the torso. Carbon fabrics were used as both electrodes. The friction generated between the sleeve and the torso produced a power density of 1.8 mW/m^2 at a frequency of 1.5 Hz. Another example, Cui et al. developed a wearable TENG with grating-structured nylon and Dacron cloth, illustrated in Fig. 2(a) [47]. The SEM image of the textile surface is shown in Fig. 2(b). A photograph of one part of the TENG is shown in Fig. 2(c) illustrating the grating structure comprising the nylon and Dacron materials. A second

identical grating is arranged on top of this to form the overall T-TENG as shown in Fig. 2(d). The gratings were fabricated on top of cotton fabric substrates with the nylon and Dacron strips being attached to the substrates with an intermediate copper (Cu) electrode. Relative sliding between the substrates, for example, when attached to the arm and body, causes that an alternating current flows between the nylon and Dacron back electrodes. With this arrangement, the I_{SC} and the V_{OC} reached a value of 0.2 mA and 2 kV, respectively.

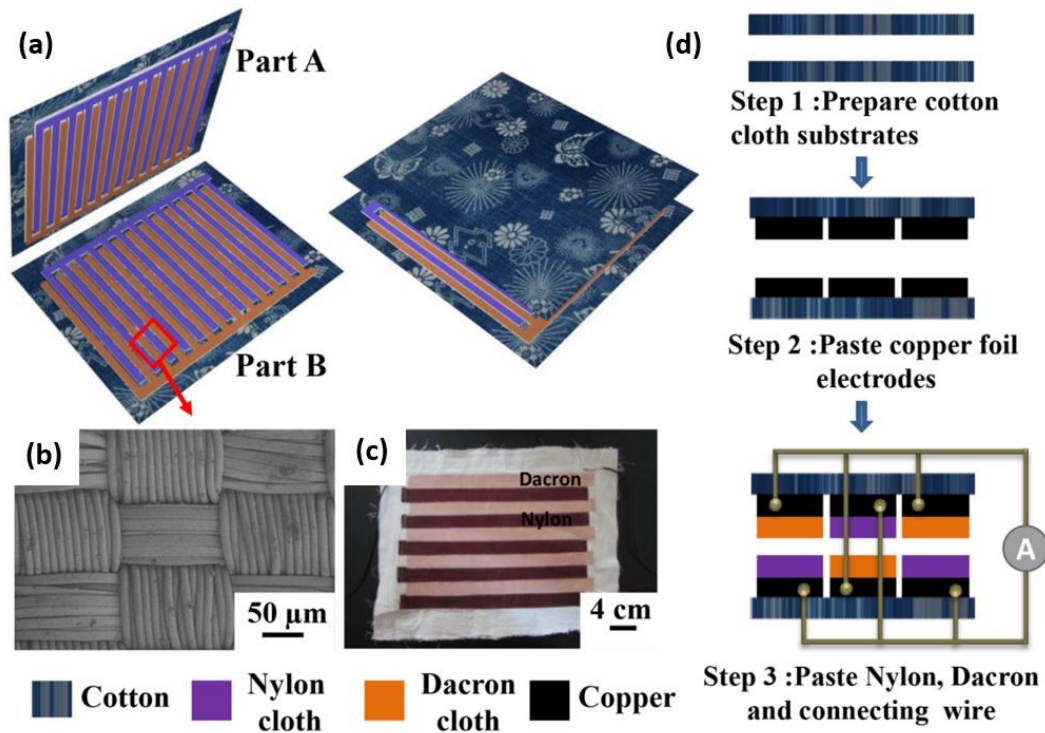


Fig. 2 (a) Schematic diagram of cloth-based TENG with a linear-grating structure, (b) SEM image of the microstructure of nylon cloth's surface, (c) photograph of one part of the TENG and (d) fabrication process of the TENG. Reprinted with permission from Ref. [47]. Copyright 2015 American Chemical Society.

2.3. Single-electrode mode (SE-mode)

The SE-mode TENG overcomes a limitation of the CS- and LS-modes that requires the moving triboelectric materials to be attached to electrodes which need to be connected to an external electrical load. The SE-mode offers the advantage of requiring only one electrode and therefore one electrical connect. The operation of the SE-mode is shown in Fig. 1(c) in which the TENG comprises only one dielectric material and one electrode. However, it should be

noted that in practical applications, a reference electrode is often connected to the primary electrode to serve as a source of electrons. The periodic vertical contact-separation movement of the dielectric causes electrons to flow between the primary electrode and the ground (or reference electrode) due to a change in the induced potential at the primary electrode. Because the potential change takes place mainly at one electrode, the output performance of this mode is lower compared to the other modes. Moreover, the primary electrode can shield the electric field between the reference electrode and the dielectric material when the electrodes are too close to each other, which results in a further decrease in the output due to a drop in the capacitance between the reference electrode and the dielectric material [48].

This mode is one of the most common operating modes for T-TENGs since the freely moving dielectric does not require an electrical connection or electrode. Consequently, it enables alternative materials to be used as a dielectric, such as conventional fabrics [49–52] or human skin [53,54]. An example of this mode was published by Lai et al. who fabricated a single-thread based wearable TENG sewn in serpentine shape on a textile as shown in Fig. 3(a) [54]. The thread was made of a stainless-steel (SS) conductive core coated with a silicone rubber (SR) shell. Via contact to and separation from the skin, the device delivered an I_{SC} of 200 μA , a V_{OC} of 200 V and a power density of 953 mW/m^2 at 1 $M\Omega$ load resistance. This power was shown to be sufficient to drive different applications, including a smartwatch, motion sensor system and wireless wearable keyboard, shown in Fig. 3(b)-(d), respectively.

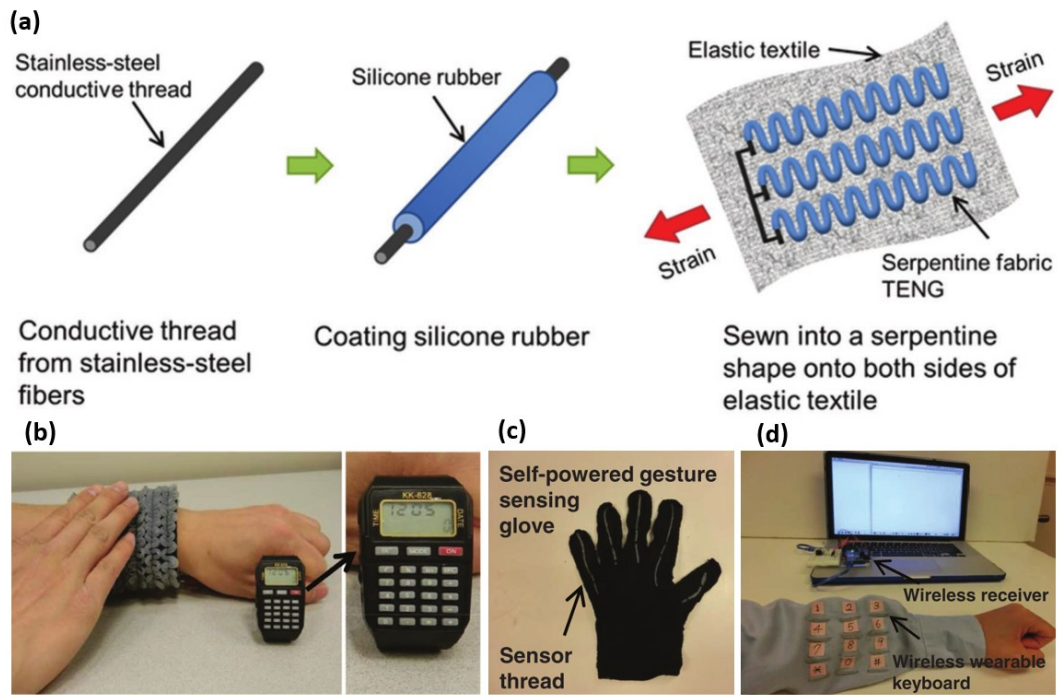


Fig. 3 (a) Schematic diagram for fabrication process of single-thread based wearable TENG in serpentine shape sewed on a textile and its applications, including (b) smartwatch, (c) motion sensor system and (d) wireless wearable keyboard. Reprinted from Ref. [54]. Copyright 2016, with permission from John Wiley & Sons, Inc.

2.4. Freestanding triboelectric-layer mode (FT-mode)

The operation of the FT-mode is illustrated in Fig. 1(d), which consists of two electrodes, aligned vertically or horizontally, and a triboelectric material. Similar to the SE-mode, the triboelectric material can move freely without electrode or electrical connection. When the triboelectric material (e.g. positive charged) is closer to one electrode, electrons will be attracted to that electrode due to a rise in the electric potential. When the triboelectric material is moved closer the second electrode, the electrons will flow from the first electrode to the second. Relative movement backwards and forwards between the electrodes results in an AC output through the external load. Compared to the SE-mode, this mode benefits from the potential change at both electrodes and there is no shielding effect [48], and therefore the performance is better. The triboelectric material can either be in contact or not with the electrodes during the operation due to the fact that the surface charge on some materials can remain for hours. For this reason, this operation mode suffers less from material abrasion and

heat generation [26]. For example, Pu et al. proposed a T-TENG consisting of a stator and a slider fabric [55]. Two interdigitated electrodes were fabricated on the stator fabric by electroless plating of nickel (Ni) and then fully covered by a parylene layer serving as a triboelectric material. The slider fabric has grating-structured segments of Ni serving as the freestanding-layer. The T-TENG with 1 mm wide segment can generate a maximum power density of 3.2 W/m^2 at a speed of 0.75 m/s . Another example of T-TENG operating in this mode was demonstrated by Yu et al. [56]. Here, a polyester (PE) textile was used as the freestanding-layer and PU/SS textiles were used as the electrodes. The T-TENG operating in this mode exhibits an I_{SC} and a V_{OC} of $1 \mu\text{A}$ and 56 V , respectively.

Most of the T-TENGs found in this mode are operated in combination with the CS-mode, this being known as the freestanding triboelectric-layer CS-mode (FCS-mode) [22,23,57,58]. The device structures comprise three triboelectric materials with the first two materials being arranged in strips with electrodes on the back or in the core. The strips (which can be fabric) are woven together forming a textile substrate. The third material, which acts as a freestanding triboelectric-layer and typically has an electron affinity between the first two materials, moves vertically in contact to and separation from the woven substrate. Based on contact electrification, positive and negative charges are generated at the surface of the first and the second materials. The periodic movement of the third material results in a potential difference between the electrodes and thus an electric power is produced. Tian et al. proposed this type of TENG using Ni-coated PE (conductive textile) and the SR-coated conductive textile as the woven substrate (shown in Fig. 4 (a)) [58]. The power generation mechanism, as described previously, is represented in Fig.4 (b). In this example, palm skin was used as the freestanding triboelectric-layer and the I_{SC} and V_{OC} of the single-layer and double-layer TENG were $60 \mu\text{A}$ and $140 \mu\text{A}$, and 500 V and 540 V , respectively. In addition to skin, the energy harvested using terylene, cotton, rubber, fur, silk and nylon as the freestanding triboelectric-layer is shown in

Fig. 4. (c)-(h), respectively. The I_{SC} for all materials exceeded $100\ \mu\text{A}$ and cotton and fur achieved over $150\ \mu\text{A}$. In Fig. 5(a), the maximum peak power of the double-layer TENG reaches $22.3\ \text{mW}$ at a load resistance of $10\ \text{M}\Omega$, corresponding to a power density of $8,920\ \text{mW/m}^2$. Fig. 5(b) shows that the output of the double-layer TENG at a frequency of $3\ \text{Hz}$ and a contact force of $300\ \text{N}$ can charge up a $22\text{-}\mu\text{F}$, $10\text{-}\mu\text{F}$, $4.7\text{-}\mu\text{F}$ and $1\text{-}\mu\text{F}$ capacitor to a voltage of $10\ \text{V}$ in $8, 28, 54$ and 120 seconds respectively.

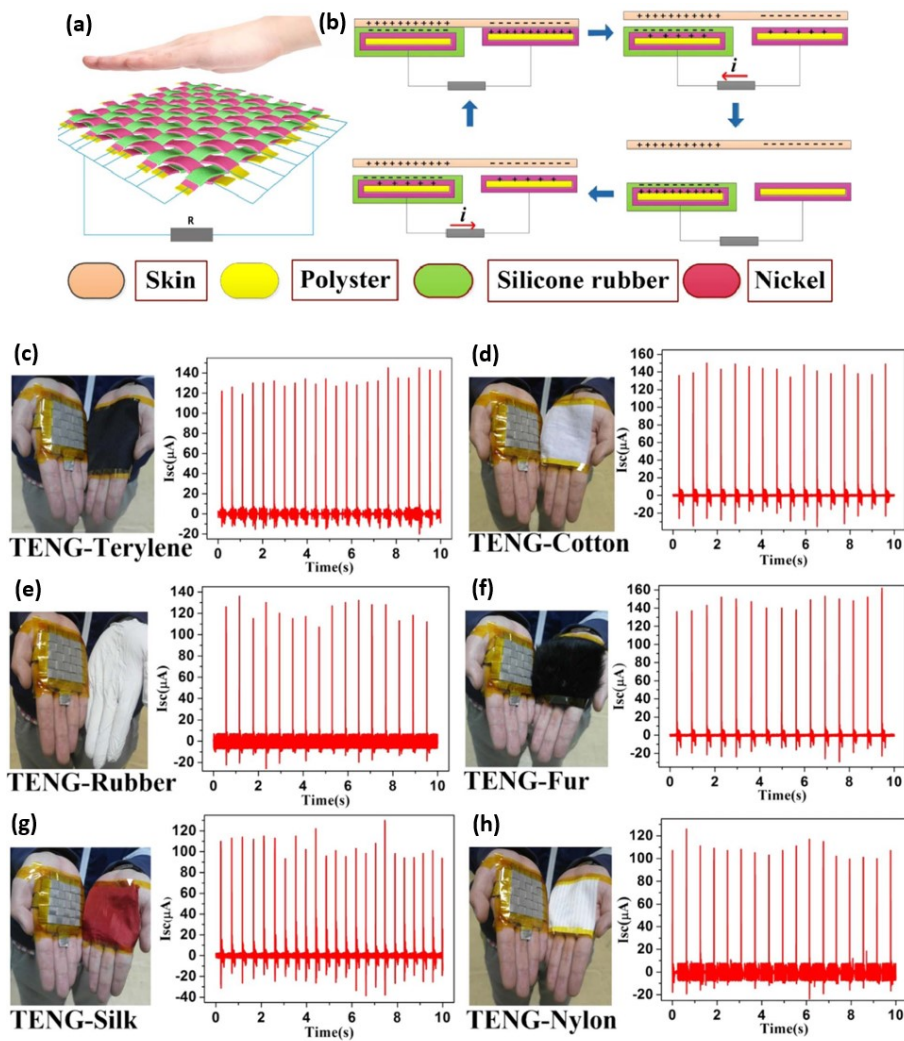


Fig. 4 T-TENG operating in freestanding triboelectric-layer contact-separation mode (FCS-mode): (a) schematic illustration and (b) power generation mechanism of the T-TENG contacted with palm skin. Photographs and the corresponding I_{SC} of the T-TENG using different materials, including (c) terylene, (d) cotton, (e) rubber, (f) fur, (g) silk and (h) nylon as the freestanding triboelectric-layer. Reprinted from Ref. [58]. Copyright 2017, with permission from Elsevier.

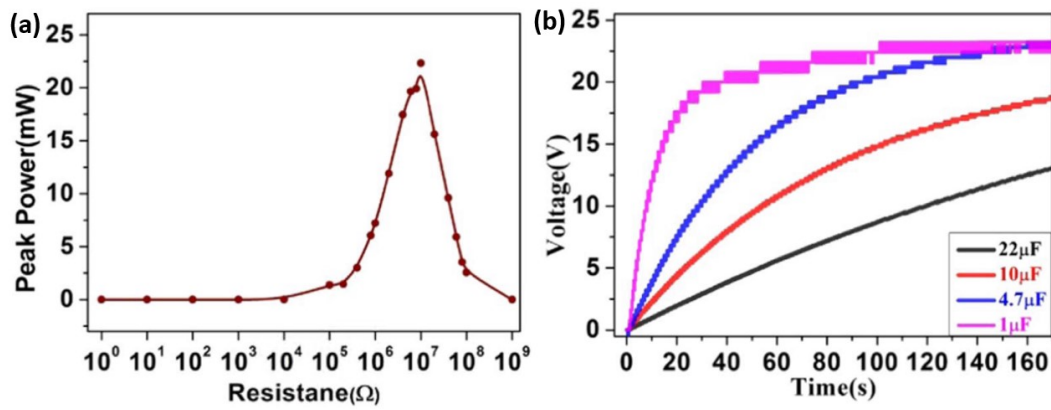


Fig. 5 (a) Dependence of the peak power of the double-layer TENG on load resistances and (b) time-dependent capacitor voltage of the different capacitors charged by the double-layer TENG. Reprinted from Ref. [58]. Copyright 2017, with permission from Elsevier.

3. Textile manufacturing

Textiles are a basic type of material that are essential for human protection and comfort. Evidence has been found indicating the existence of textiles goes back more than 20,000 years [59]. Since the Industrial Revolution, textile manufacturing has developed in all aspects, including technique, cost, quality and throughput. With regard to T-TENGs, textile production techniques and its structure can have a considerable impact on its performance. Therefore, it is important to pay attention to the basic fundamental of fabric manufacturing.

Fabrics are made from yarns that are typically composed of spun fibres. Two essential dimensional features of fibres are their fineness and length. Flexibility stems from fineness and length provides coherence. Fineness is often expressed by linear density using an SI unit called tex (g/km). The linear density of fibres typically varies between 0.1 and 2 tex [60]. The length of fibres can be only a few centimetres (staple fibres) or several kilometres (filament fibres) and it is typically several hundred times the diameter. The diameter of fibres typically ranges from ten to several hundred micrometres. Fibres can be classified into two main categories: natural and man-made. Natural fibres stem from animals (wool, silk, hair), plants (cotton, linen, hemp) and minerals (asbestos, glass fibre). Animal and plant fibres are typically soft, breathable, absorbent and biodegradable, however, they can shrink in hot water, wrinkle easily

and some of them can irritate the skin. Man-made fibres can be divided into two groups, namely cellulosic and noncellulosic. Cellulosic fibres are regenerated fibres made from natural materials, which are chemically processed, for instance, rayon and acetate. Noncellulosic fibres are synthetic polymer fibres made by refining crude oil or coal e.g. nylon, PE and acrylic. Man-made fibres are typically durable, lightweight, inexpensive and quick drying but can have reduced breathability and biodegradability. Yarns are long continuous strands produced by spinning the fibres together. When two or more yarns are twisted together, they are known as ply yarns. Different fibres require different preparation processes before they can be spun into yarns. In case of cotton, the world's most important natural fibre, its standard processes are opening, cleaning, blending, carding, combing, drafting, twisting and winding [61].

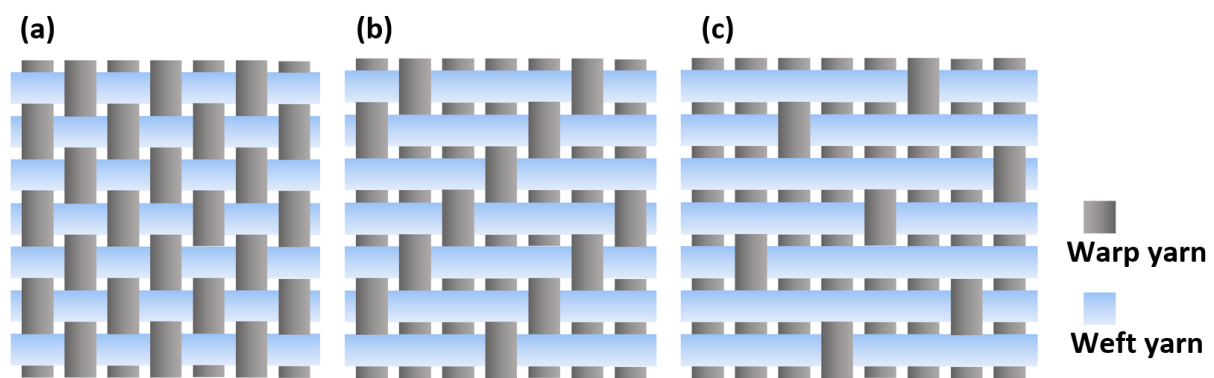


Fig. 6 Three basic weaves: (a) plain weave (b) twill weave and (c) satin weave.

Textiles are formed by interlocking yarns together by, most commonly, weaving using a hand or power loom and knitting using knitting needle, crochet hook or knitting machine. Woven fabrics are made by interlacing warp yarns (vertical yarns) and weft yarns (horizontal yarns). Different weaving techniques can achieve a diverse range of fabric structures. Three basic weaves are used for the majority of two-dimensional (2D) fabrics, these being plain, satin and twill as shown in Fig. 6(a)-(c). Other weaving structures include basket, pile, crepe jacquard, ribbed, braided and triaxial woven [61,62].

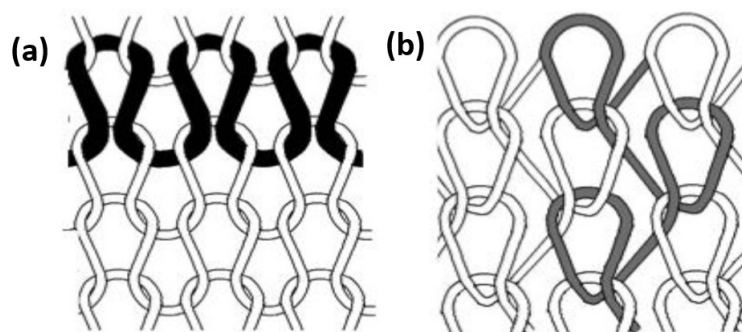


Fig. 7 Two basic knitted structures (a) weft knitting and (b) warp knitting. Reprinted from Ref. [4]. Copyright 2017 with permission from the authors, MDPI.

Knitted fabrics are produced by forming interlocking loops of yarn. The horizontal row and each vertical row of loops are known as the course and wale, respectively. There are various ways of looping, which generate two main types of knitted fabric known as weft and warp knitting. Fig. 7(a) represents weft knitting with one continuous yarn forming courses across the fabric and Fig. 7(b) shows warp knitting with series of yarns forming wales in the vertical direction [63]. Other knitting processes include Raschel, crochet, Milanese, fleece, and terry knit [61]. There is also a class of fabrics known as non-woven that have a web like structure made up of short fibres that are held together by various techniques, including needling, knitting, stitching, thermal and chemical bonding. Examples of the common non-woven fabrics are felted fabrics that are produced by pressing wool or fur under a certain pressure, moisture and heat and bonded fabrics that are produced by bonding fibres together using methods such as stitching or adhesion. The electrospinning method can also be utilized to make nanofibre-based non-woven fabrics. An electric field is used to draw charged threads towards a grounded collector from polymer solutions or melts thereby forming fine fibres with diameters ranging from 2 nm to several micrometres. The properties of non-woven fabrics produced by this technique can be adjusted (e.g. porosity) and can achieve a much denser structure with a higher surface-to-volume ratio compared to conventional techniques [64,65].

Three-dimensional (3D) fabrics can also be manufactured by weaving, knitting, braiding, stitching and non-woven methods. The simplest form of 3D fabric is made up of 2D fabrics

that are stacked on top of each other and bound together in the thickness direction using the techniques, such as stitching, needle-punching, chemical bonding or lamination. 3D woven structures can be realised using multiple yarns sets including a z-yarn aligned through the thickness of the fabric. The weaving process is performed both in-plane and out-of-plane directions. Although through-the-thickness fibre reinforcement improves out-of-plane properties of 3D woven composites, in-plane mechanical properties are generally low. 3D knitted fabrics are produced by the 3D spatial formation of 2D warp or weft knitted fabrics. Due to their characteristic looped architecture and low fibre volume fraction, the mechanical properties are reduced. The 3D fabrics are often utilised as reinforcement materials in various fields, such as civil engineering and military industry [62].

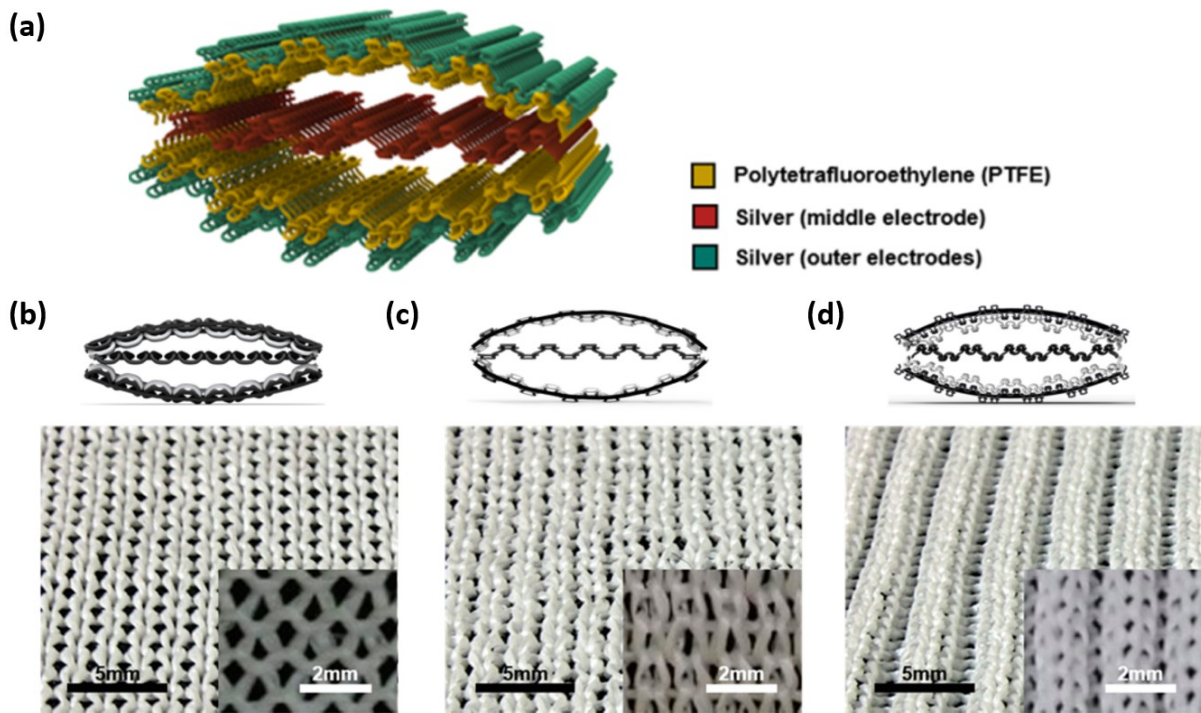


Fig. 8 T-TENG with three different knitted structures: (a) Schematic illustration of the T-TENG, (b) plain-knitted structure, (c) double-knitted structure, and (d) rib-knitted structure with insets of the magnified photos. Reprinted with permission from Ref. [66]. Copyright 2017 American Chemical Society.

The effect of fabric structure on the performance of T-TENG was demonstrated by Kwak et al. [66]. As shown in Fig. 8(a), polytetrafluoroethylene (PTFE) yarns and silver (Ag) yarns were knitted together forming stacks of two PTFE triboelectric layers, one Ag inner electrode

and two Ag outer electrodes. This work investigated the performance of plain-, double-, and rib-structure weft-knitted fabrics (illustrated in Fig. 8(b)-(d)). Under a cyclical compressive force, an alternating current between the Ag inner electrode and outer electrodes was obtained. The study showed that the TENG with rib-knitted structure exhibited the maximum effective contact area and stretchability. As a consequence, it produced a V_{OC} of 23.50 V, which is more than ten times and almost two times greater than the double- and plain-structures, respectively.

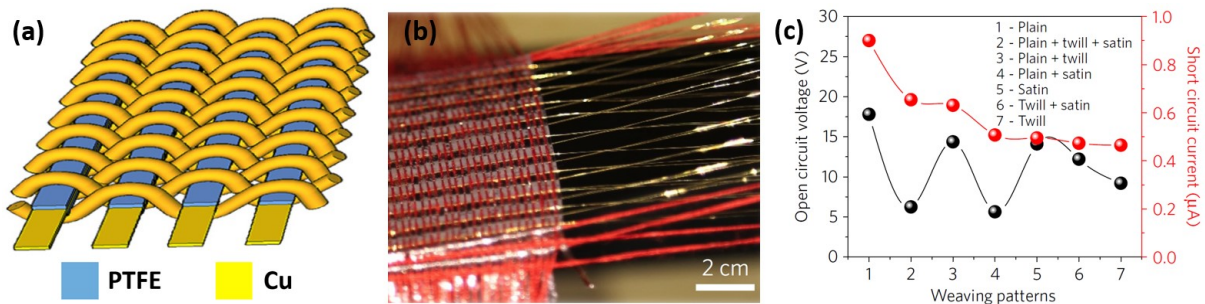


Fig. 9 (a) Schematic illustration of T-TENG with plain weaving structure, (b) photograph of the textile weaving process and (c) dependence of the electrical output on the different woven structures. Reprinted with permission from Ref. [67]. Copyright 2016 Nature Energy.

Chen et al. have confirmed the importance of the textile structure [67]. They demonstrated a hybrid harvester comprising photovoltaic textile and T-TENG. The electrical output of the T-TENG woven from PTFE strips and Cu fibres varies depending upon the variation in the effective contact area relating to the string-packing density in the different woven structures. Fig. 9(a) shows a schematic illustration of the T-TENG with a plain weaving structure. The photograph in Fig. 9(b) reveals the textile weaving process and Fig. 9(c) shows the dependence of the electrical output generated via hand clapping on the different woven structures. From the three basic woven structures, the T-TENG with plain weave produces the highest power, followed by satin and twill weave, while the output of the TENGs with mixed woven structures lies between the corresponding basic structures.

4. Materials

There is a limited range of materials that possess the mechanical and electrical properties necessary to be used in a T-TENG. The desirable properties are, for example, flexible, stretchable, biocompatible, light, durable, washable and breathable. The materials can be sorted into two following major groups.

4.1. Triboelectric materials

Triboelectric materials are the materials on whose surface the triboelectric effect takes place when they are brought into contact with each other. The choice of triboelectric material plays a fundamental role in the output performance of the T-TENG. The individual properties of materials, such as the electron affinity and the work function, can determine the polarity and the charge density of materials. A guideline for material selection is the triboelectric series [68], which is a list of various materials sorted by their tendency to lose or gain electrons. For example, a material at the top of the list will lose electrons and be positively charged when rubbed against a material at the bottom of the list that will receive electrons and become negatively charged. The further apart in the list the two materials are, the greater the tendency for electron transfer. For this reason, a TENG should consist of at least two materials, which are separated as far as possible on the list. Theoretically, each material can become either positively or negatively charged depending on the triboelectric property of the material it makes contact with. However, there are certain choices of materials for T-TENG, which are typically selected as the positive or negative triboelectric materials. Metal, including Al, Cu, Ni, and silver (Ag), are often used as the positive triboelectric materials because they are at the top of the triboelectric series and can also be used as an electrode at the same time. Most textiles, such as nylon, cotton and silk also tend to become positively charged and PU is the most positive material in the triboelectric series. Typical negative materials are PDMS, parylene, polyvinylidene fluoride (PVDF), silicone rubber, PTFE and fluorinated ethylene propylene

(FEP). These materials are often coated on fibres or textiles to improve the triboelectric properties of T-TENGs [69,70].

4.2. Electrode materials

Electrodes are essential parts of T-TENG. They are electrical conductors where the electrostatic induction takes place. Poor electrical properties, such as low carrier mobility, and low free carrier density can lead to a considerable energy loss in the materials and thus a reduction in the efficiency of the TENG. In this section, different techniques to achieve conductive and flexible electrodes suitable for T-TENGs will be discussed.

4.2.1. Metal-based electrode

The simplest metal-based electrode is made of metal foil [31,47]. It can be attached to the triboelectric textile materials with adhesive or double-sided adhesive tape. This type of electrode benefits from high electrical conductivity but the assembly is prone to failure after cyclical bending and they are not stretchable or breathable. Furthermore, the additional thickness arising from the adhesive layer causes a drop in the potential difference and a corresponding reduction in performance of the TENG [71,72]. The more popular approach is to utilise metal-based conductive fabrics (CF). A metallic thin film can be deposited on fabric using standard microfabrication processes, such as sputtering [49] or evaporation [52]. The disadvantages of these methods include incompatibility with large-scale textile manufacturing processes, high cost of production, unsuitability for complex surface topologies and porous fibres and lack of mechanical durability [73]. Alternatively, the metal layer can be deposited using electroless plating. For instance, a Ni-coated PE fabric has been prepared by immersing PE cloth into NiSO₄ aqueous solution [57]. Another technique is to introduce metallic nanoparticles (NPs) or nanowires (NWs) on textiles. For example, Lee et al. demonstrated polymer/Kevlar coated with silver nanoparticles (AgNPs). It exhibited a good mechanical stability after 3000 bending and a low resistivity of 0.15 Ω/cm [74]. Besides, Guo et al.

successfully fabricated conductive fabric by dip-coating nylon cloth with a solution of silver nanowires (AgNWs). Their T-TENG with AgNWs electrode was used as a personal energy management device for wearable applications [31]. Nevertheless, the resistance of these examples is likely to increase with stretching and conductive particles can be removed during washing reducing conductivity and potentially polluting the environment [75]. Resistance to the effects of stretching can be improved by, for instance, covering a stretched substrate surface with NWs to create buckled conductive layer after release [41,76,77] or adding a supplemental material such as graphene [35] or 3-aminopropyltriethoxysilane (APTES) [78] to the NWs layer. Most recently, Yang et al. has demonstrated a liquid-metal-based TENG by injecting Galinstan into SR fibres, which enables Galinstan electrodes to remain conductive even when stretched. The TENG successfully demonstrated its suitability for powering wearable devices, such as pedometer, minicalculator and electronic watch [79]. For fibre-based TENGs, metal fibres are often used as electrodes. They can simply be spun into yarns and/or woven with other commercial yarns using standard industrial processes. This technique provides the opportunity for the mass production and commercialisation of T-TENGs [56,67].

4.2.2. Carbon-based electrode

Carbonaceous materials such as carbon nanotubes (CNTs), carbon nanoparticles, carbon fibres and graphene are promising for the use as electrodes in T-TENG. According to Zeng et al., they possess high intrinsic carrier mobility ($10^6 \text{ cm}^2\text{V}^{-1} \text{ S}^{-1}$), high electrical conductivities (10^4 S/cm), excellent mechanical properties (elastic modulus in the order of 1 TPa) and environmental stability [80]. CNTs are the most widely used carbon-based materials for T-TENG due to the simple fabrication process and low fabrication cost [73]. The common technique used is called “dipping and drying” by which fabric [51] or yarn [81] is immersed in a conductive ink solution containing single-wall or multi-wall CNTs (MWCNTs). Graphene is a form of carbon comprising a single layer of carbon atoms arranged in a hexagonal lattice.

Recently, Chu et al. published research on a graphene-based TENG where the electrode was formed from ultrathin double-layer graphene with a thickness less than 1 nm grown by thermal CVD. Its potential application as a self-powered conformal touch sensor was also illustrated [82]. Another graphene-based T-TENG was demonstrated by Zhu et al. with one of the electrodes fabricated from nylon fabric coated with graphene ink [83]. Despite the advantages, carbon-based T-TENGs still have not been commercialised yet because of difficulties in scale-up and the high cost of the materials [23].

4.2.3. Polymer-based electrode

Conductive polymers are a promising material for wearable electronics due to their inherent flexibility and environmental stability. However, the major drawback is the low conductivity. Shirakawa et al [84] introduced the first conductive polymer by exposing polyacetylene (PA) polymer to iodine vapour and achieved a conductivity of 30 S/cm. Nowadays, the most intensively explored conductive polymers are polypyrrole (PPy) and poly-(3,4-ethylene dioxythiophene) (PEDOT). PPy is commonly synthesized by electrochemical polymerisation [85,86]. The conductivity of PPy stems from the coupling between the electron transfer along the conjugated π -molecular orbital backbone and the motion of charge carriers. However, due to its poor insolubility, large-scale fabrication is limited [87]. PEDOT is a conductive polymer with high conductivity resulting from its unique structure, which comprises dioxyalkylene bridging groups at positions 3 and 4 of its heterocycle ring [73]. Conductivity can be regulated from 10^{-4} to 10^3 S/cm [88]. Sutka et al. demonstrated that PEDOT can be used as both a triboelectric and an electrode material for TENG, which produced ~ 3 times more power density than TENG with indium tin oxide (ITO) electrodes [89]. Similar to PPy, PEDOT is insoluble but when doped with polystyrene sulfonate (PSS), PEDOT:PSS becomes highly soluble in water. This opens up new processing possibilities such as dipping and drying, and vacuum

filtration. The latter is exemplified in the work of membrane-based flexible T-TENG undertaken by Das et al [34].

5. Surface modification

5.1. Topographic modification

Another factor that strongly determines the performance of a TENG is its nano/microscopic surface roughness. Various methods have been applied to form different micro or nanostructures on the surface, for example, pyramids [30,90], NWs [33,39] and NPs [91–93]. These structures can be formed by standard microfabrication processes such as etching or thermal deposition. In the case of standard TENGs, several investigations have been reported. For example, Fan et al. investigated the effect of different surface patterns on the performance of a TENG by introducing arrays of lines, cubes and pyramids on PDMS films using a silicon mould [94]. The PDMS film was attached to a polyethylene terephthalate (PET)/ITO substrate to form a CS-mode TENG. They found that the maximum output performance was obtained from the TENG with the array of pyramids, followed by cubes, lines and no array, respectively. The results revealed an almost four times improvement in the performance of the pyramids-structured TENG compared to the TENG with no arrays. Similarly, Jeong et al. studied the effect of nanodots, nanogrates and nanomeshes patterned silica surfaces on the performance of a PTFE/Silica TENG [95]. The results showed that the power output of the nanomesh patterned TENG was 6.3 times higher than that of the plain TENG. Zhang et al. reported that the combination of micro/nano dual scale patterns on the PDMS film enhanced the current and voltage output of the TENG by 157% and 100%, respectively [96]. Focusing on T-TENGs, Lee et al. used textiles as the top and the bottom substrate with the top textile coated with AlNPs using thermal evaporation, and the bottom textile with spin-coated PDMS [92]. The PDMS was then etched using RIE to form NWs on the surface. With this approach, a very high instantaneous power density of 336 W/m^2 was obtained at an external load of $20 \text{ }\Omega$. Ko et al.

investigated the effect of different nanostructures on the performance of T-TENG [97]. The device comprised nano-structured conductive bundle yarns (CBYs) serving as positive triboelectric material and PDMS serving as the negative triboelectric material. They found out that the growth of zinc oxide (ZnO) NWs coated with ZnO NPs on the CBY surface increased the power density of the T-TENG by approximately 45 times and 8 times compared to plain CBYs and CBYs with only ZnO NWs, respectively.

5.2. Chemical modification

In contrast to the topographic modification, which usually involves additional physical fabrication processes, the chemical modification process is simpler and can be performed without new substrate design. In this case, the substrate will be commonly covered with an ultrathin layer of molecules containing fluorine. The fluorine atom has a very high ionisation energy, and therefore the electron binding energy of the substrate increases and the treated surface will tend to gain electrons rather than to lose them. Zhang et al. demonstrated that the fluorocarbon plasma treatment of the surface of PDMS enhanced the output power of a TENG by 278% [98]. Song et al. engineered molecularly surface of PDMS in TENG by self-assembled monolayers (SAMs) [52]. First, the PDMS surface was exposed to an oxygen plasma to form hydroxyl groups. Subsequently, SAMs containing different end-functional atoms were deposited on the PDMS surface by either liquid-phase or vapor-phase deposition method. The results showed that the TENG with SAM containing end-fluorine atoms exhibited the best output performance with an I_{SC} of 27 μA , a V_{OC} of 105 V and a power density of 1.8 W/m², which is more than 60 times higher than that of an unmodified TENG. T-TENGs fabricated from fabrics such as silk, cotton, and PET (Dacron) with surface modification by SAMs were also represented in their research. The modified fabrics were brought into contact with a PET/ITO film. While the V_{OC} of the T-TENG with Dacron increased from 25.7 V to 42 V, the values for the silk and the cotton decreased from 54.7 V and 35.7 V to 23.1 V and 20.6

V, respectively, due to a decline in the triboelectric charge gap between the fabrics and the PET/ITO film in the triboelectric series.

6. Material and structural design

There are numerous example T-TENGs in the literature and the following review has been categorised into two main groups, fabric-based T-TENG and fibre-based T-TENG.

6.1. Fabric-based T-TENG

Fabric-based T-TENGs are the most common type of T-TENG due to its relatively straightforward fabrication process and high electrical output. It is composed of conventional fabric, which can either be directly used as a triboelectric material and/or just serves as a substrate.

6.1.1. Fabric-based T-TENG using the fabric as triboelectric layer

In this case, fabric is used as one or both of the triboelectric materials. It can be a fixed part of T-TENG or can only serve as the freestanding-layer in FT-mode, FCS-mode and SE-mode. For example, Chu et al. demonstrated a conformal ultrathin T-TENG operating in the SE-mode [82]. Fig. 10(a) illustrates its structure, which is composed of a thin PET layer ($<0.9\ \mu\text{m}$), graphene ($<1\ \text{nm}$) and PDMS ($<1.5\ \mu\text{m}$) serving as the substrate, the electrode and a triboelectric material, respectively. The PDMS surface was nanostructured by O_2 plasma etching and chemically modified by SF_6 plasma and these treatments increased the output current and voltage by a factor of more than 10. Due to its thickness and flexibility, the device could be applied to human skin and used to generate power when the PDMS comes into contact with the cloth. Different types of fabric, including nylon, silk, cotton and latex were tested as triboelectric materials. It was found out that the effective contact area, which varied from 21% to 98% of the total contact area, was related to the woven structure of the fabrics and the V_{OC} and I_{SC} ranged from 16.3 V to 30.9 V and 1.9 μA to 3.9 μA respectively, as illustrated in Fig.

10(b). By dint of a hand tapping with a nitrile glove, the device generated a maximum V_{OC} , I_{SC} and power density of 47.1 V, 7 μA and 144 mW/m^2 , respectively.

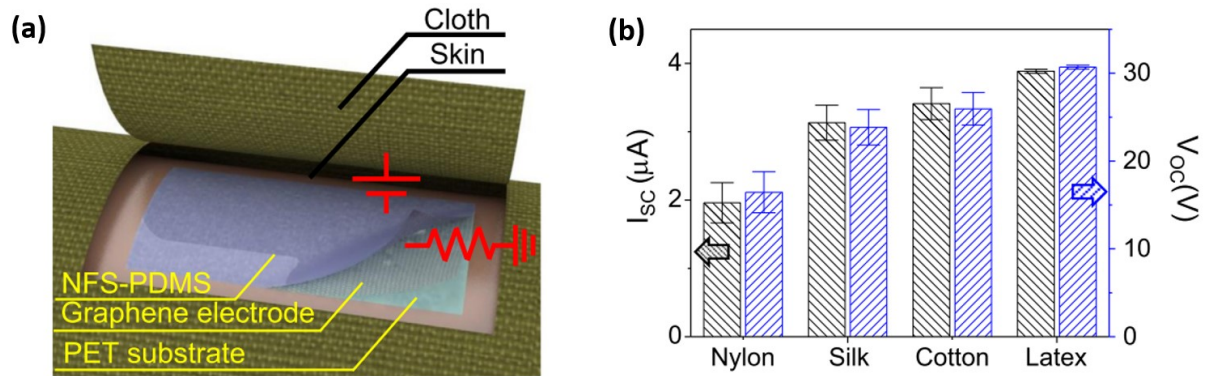


Fig. 10 (a) Schematic illustration of conformal ultrathin T-TENG and (b) I_{SC} and V_{OC} of the conformal T-TENGs for different types of fabric tested as triboelectric materials. Reprinted from Ref. [82]. Copyright 2016, with permission from Elsevier.

One simple way to fabricate this type of T-TENG is to use the fabric as a triboelectric layer and coat one surface of the fabric with a conductive material to collect the induced charges. With this concept, Zhu et al. designed a 3D spacer fabric-based T-TENG consisting of three layers: two outer nylon weft-knitted fabric layers and a PE spacer layer [83]. The upper surface of the nylon layer was coated with a graphene ink to form the electrode and the lower nylon fabric layer was coated with PTFE. When the TENG was periodically pressed and released, charge separation occurred at the surface of the nylon fabric and PTFE coated nylon fabric leading to charge induction at the electrodes. A power density of 53.3 mW/m^2 was obtained at a frequency of 1 Hz and an external load of 0.6 $M\Omega$.

A good example of T-TENG, which can operate in a lateral stretching and release mode was reported by Choi et al. They designed a T-TENG with a corrugated structure, shown in Fig. 11(a) [99]. The top layer was produced by backstitching silk with a woven conductive fabric (Sn/Cu/Ag-plated nylon). The bottom layer was made of a knitted conductive fabric (Ag-plated nylon) coated with silicone rubber. Then, the corrugated top layer was sewn on the bottom layer. As shown in Fig. 11(b), the triboelectric effect arose from the contact-separation

between the silk and the silicon rubber during stretching and release. A maximum V_{OC} , I_{SC} and power density of 28.13 V, 2.71 μA and 166 mW/m^2 could be reached, respectively.

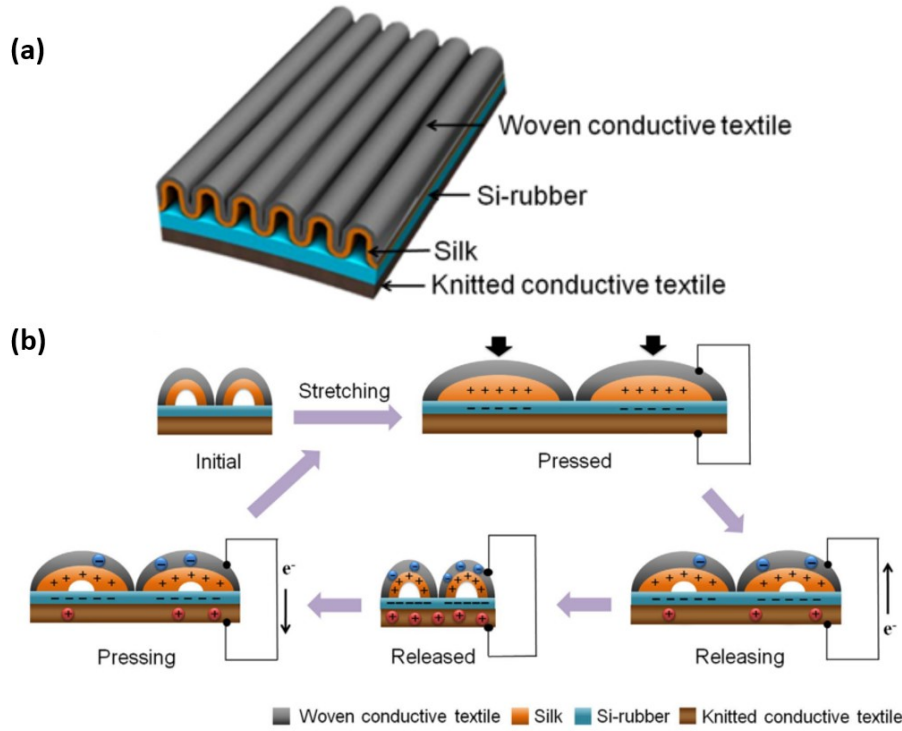


Fig. 11 (a) Schematic illustration of T-TENG with a corrugated structure and (b) power generation mechanism via stretching and releasing. Reprinted from Ref. [99]. Copyright 2017 with permission from the authors, Nature.

6.1.2. Fabric-based T-TENG using fabric as substrate

In many example T-TENGs, the fabric only serves as one or both substrates i.e. they provide mechanical support and another material with better triboelectric properties is attached to the textile. Because of this, the material choice and the performance of the T-TENG can be significantly increased. A simple method to fabricate this type of T-TENG was demonstrated by Pu et al. [23]. The T-TENG was fabricated by plain-weaving stripes of Ni-coated PE fabric (Ni-cloth) and parylene-coated Ni-fabric (P-Ni-cloth) as shown in Fig. 12(a). The conductive Ni-cloths, which serve as both electrodes, were produced by electroless plating of Ni on the PE cloths, whereas the P-Ni-cloths were coated by CVD deposited parylene. The power generation mechanism is demonstrated in Fig. 12(b). The contact-separation between two TENG cloths under repeated force lead to a charge separation between the Ni-cloths and the P-Ni-cloths and

an alternating current flow between their electrodes. The resultant T-TENG fabric largely maintained the flexibility, the washability and comfort of the PE cloth. In CS-mode, the power cloth could produce a power density of up to 393.7 mW/m^2 at a frequency of 0.7 Hz and a load resistance of $70 \text{ M}\Omega$.

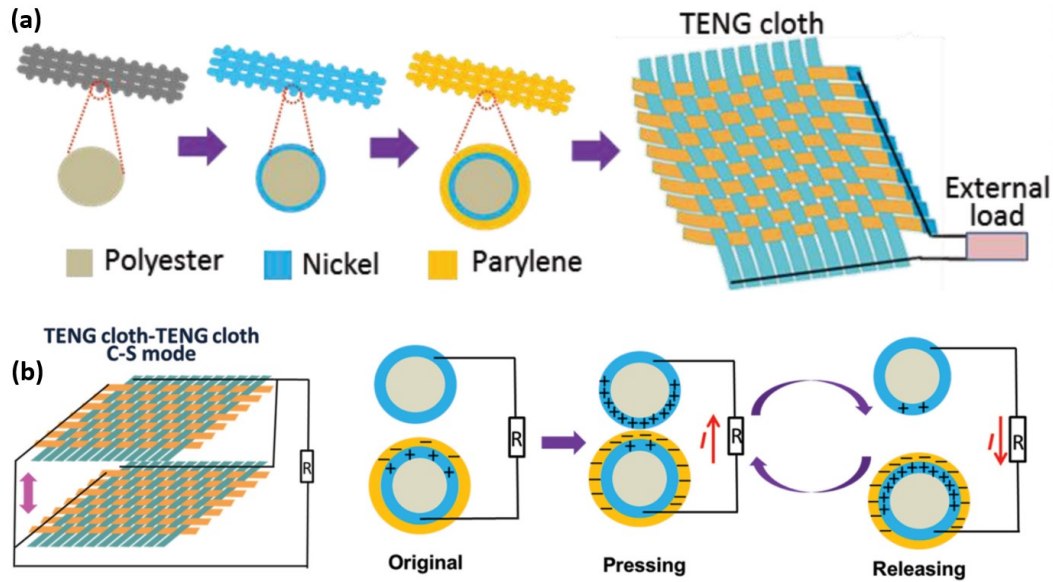


Fig. 12 (a) Schematic illustration of T-TENG fabricated by plain-weaving stripes of Ni-cloth and P-Ni-cloth, and (b) power generation mechanism via a repeated compressive force. Reprinted from Ref. [23]. Copyright 2015, with permission from John Wiley & Sons, Inc.

A more complex T-TENG structure was proposed by Liu et al. [30] who used a 3D spacer PET fabric with a three-dimensional structure. One surface of the fabric was coated with PDMS forming a pyramid-structured surface combined with a CNT sheet electrode and the other surface was coated with Ag to act as an electrode. By means of a contact-separation movement through a repeated compressive force, opposite charges were generated on PET and PDMS surfaces causing a current flow between the Ag and CNT electrode. This T-TENG produced V_{oc} , I_{sc} and power density of 500 V , $20 \mu\text{A}$ and 153.8 mW/m^2 , respectively. It was also shown that there is no significant change in the performance after 3000 cycles of pressing and releasing.

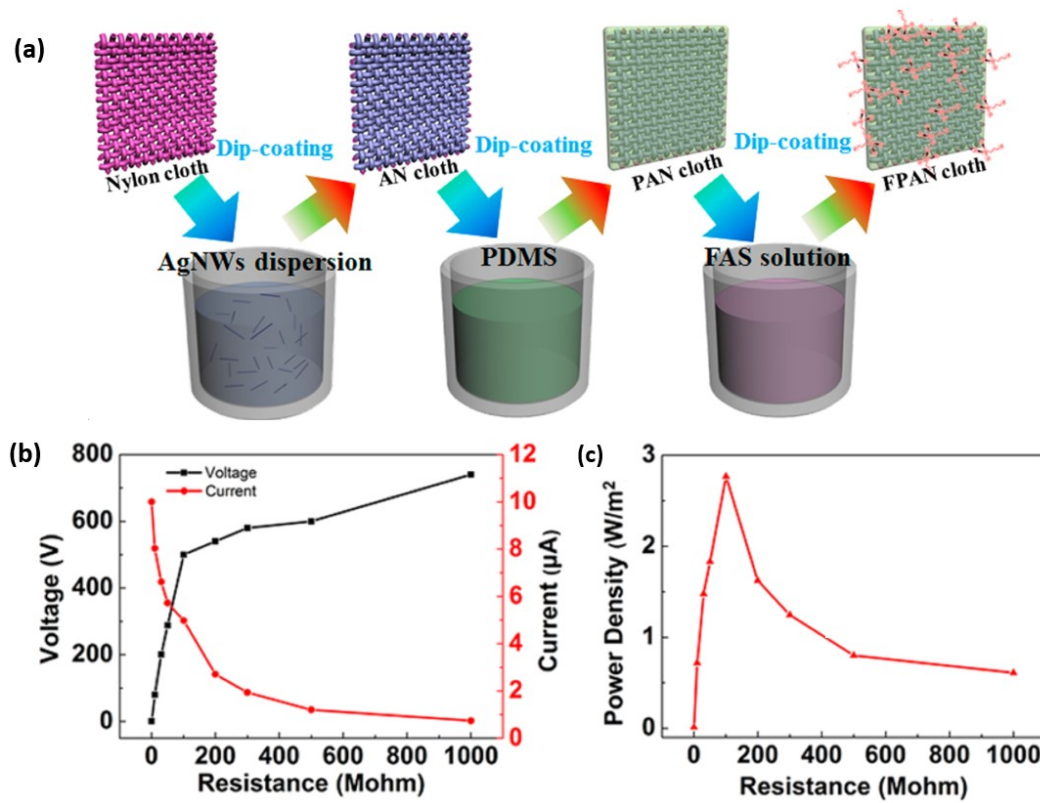


Fig. 13 (a) Schematic diagram of the fabrication process of the fabric-based TENG proposed by Guo et al.. Load resistance dependence of (b) peak output voltage and current, and (c) corresponding instantaneous power of the TENG. Reprinted with permission from Ref. [31]. Copyright 2016 American Chemical Society.

A high-performance T-TENG was demonstrated by Guo et al. in 2016 [31] who used a nylon cloth as the substrate dip-coated with AgNWs, PDMS, and fluoroalkyl silane (FAS) in sequence. The fabrication process is presented in Fig. 13(a). The AgNWs, PDMS, and FAS layer functioned as an electrode, a triboelectric material and the chemically modified surface, respectively. The other electrode was composed of a commercial PET cloth, double sided tape and Al foil electrode. The addition of the FAS layer resulted in increased V_{OC} and I_{SC} from 53.2 V to 575 V and 1.1 μA to 12.1 μA compared to the device without the FAS layer. The load resistance dependence of the electrical outputs is shown in Fig. 13(b) and the electrical power output is given in Fig. 13(c), which shows a clear peak of 2.77 W/m^2 at a load resistance of 100 M Ω . Furthermore, this T-TENG showed an increase in thermal insulation by 8% and good durability after 12000 test cycles.

6.2. Fibre-based T-TENG

Fibre-based T-TENG consist of one single or multiple fibres, which can partly or fully function as TENG and can be later woven or knitted into fabric. Based on its structure and energy harvesting capability, fibre-based T-TENGs can be divided into three groups, namely single-thread semi-integrated T-TENG, single-thread fully-integrated T-TENG and multiple-thread fully-integrated T-TENG.

6.2.1. Single-thread semi-integrated T-TENG

Single-thread semi-integrated T-TENG is a TENG which is in the form of a thread. It is typically composed of a conductive core and a dielectric shell. The stand-alone thread cannot produce electricity by itself but requires contact with an external triboelectric material. To increase the electrical output from a textile, several threads can be interlocked and their electrodes can be connected together. Dong et al. published their work about all-yarn-based T-TENG [100]. They fabricated a fabric from threads made of semi-integrated T-TENG using the weft-knitting technique. Each thread comprised a three-ply spun SS/PE fibre blended yarn in the core and silicon rubber in the shell. By contacting with an acrylic plate in the SE-mode at a frequency of 3 Hz, a load resistance of 100 M Ω and a contact force of 11 N, the T-TENG generated a power density of 85 mW/m². Furthermore, it showed no considerable degradation in the performance after 50,000 contact-separation cycles and 15 washing cycles.

A commercially viable T-TENG was represented by Yu et al. [56] who developed a T-TENG fabrication process, which is compatible with the standard industrial processes for mass production of textiles. As shown in Fig. 14(a) and (b), a commercial machine was used to twist natural or man-made fibres around conductive fibres resulting in core-shell yarns. Afterwards, the yarns could be woven or knitted into fabric by ordinary textile manufacturing. The resultant fabric exhibited very similar physical properties to conventional fabric being flexible, comfortable, washable and durable. The operations of the T-TENG in the SE-mode, CS-mode,

and FT-mode are illustrated in Fig. 14(c). The maximum power of 60 mW/m^2 was achieved in the SE-mode when SS, PU and PE were used as the core fibres, the spun man-made fibres and the external triboelectric material, respectively. Note, only the T-TENG operating in SE-mode belongs to single-thread semi-integrated T-TENG, whilst the T-TENG operating in CS- and FT-mode are classified into multiple-thread fully-integrated T-TENG, which will be discussed in detail later.

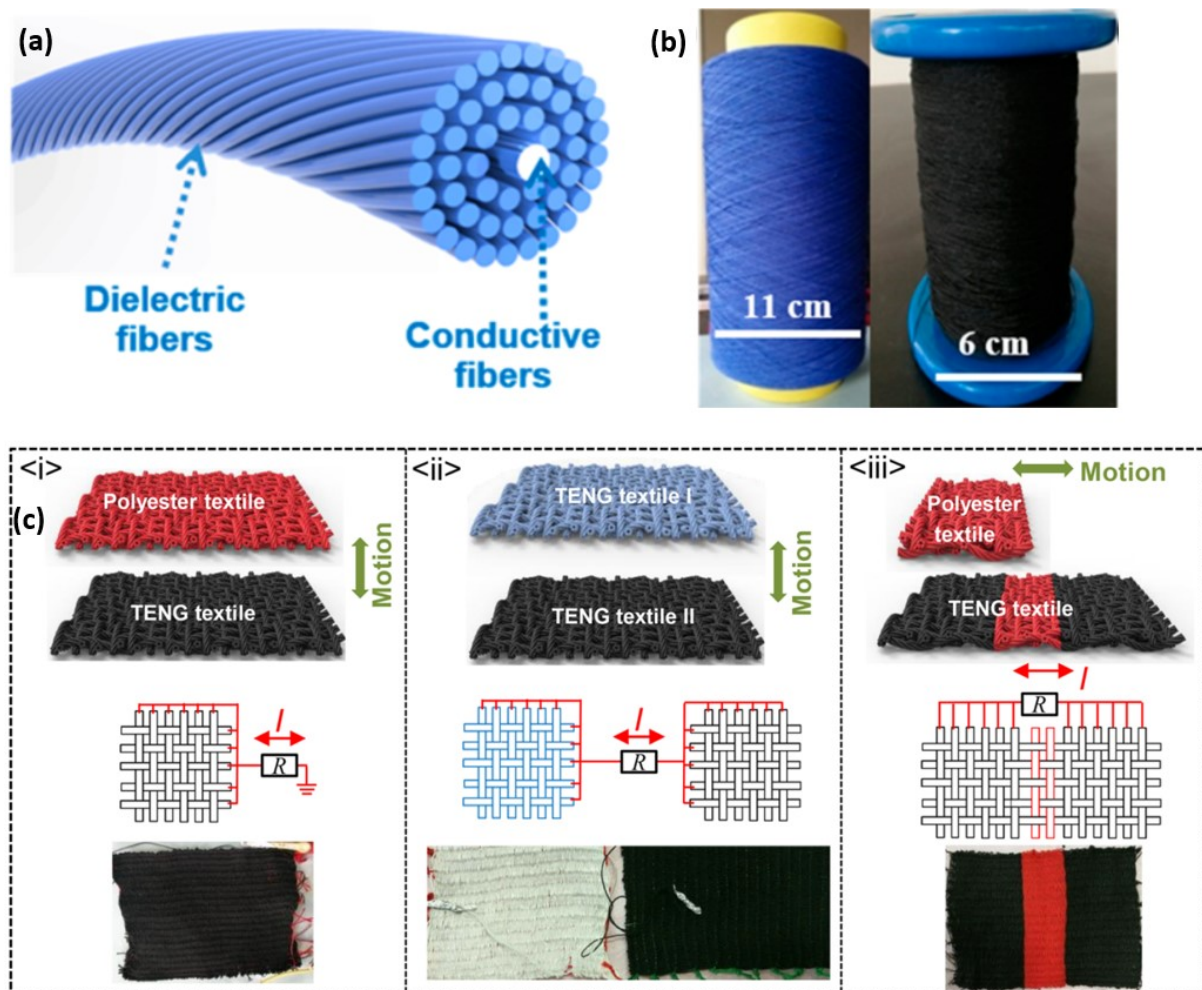


Fig. 14 (a) Schematic illustration of core-shell yarns, (b) industrialised Spandex/SS core-shell yarns with different colours and (c) three possible operation modes of the T-TENGs: i. SE-mode, ii. CS-mode and iii. FT-mode. Reprinted with permission from Ref. [56]. Copyright 2017 American Chemical Society.

As shown in Fig. 15, a fibre-based hybrid nanogenerator combining a SE-mode semi-integrated TENG and piezoelectric nanogenerator (PENG) was realised by Li et al [101]. The PENG in the core was made from carbon fibre and ZnO NWs wrapped by a nylon film, which

was coated with Ti/Cu on both sides. The inner Ti/Cu layer acted as an electrode for the PENG. The fibre was finally dip-coated with PDMS. The PDMS and the outer Ti/Cu layer served as the triboelectric layer and the electrode. A nylon fibre was chosen as the external material for contacting the T-TENG and pressing the PENG at the same time. The power density of the T-TENG and the PENG reached 42.6 and 10.2 mW/m², respectively. In addition, five fibres of the generator were woven with cotton thread to form a power suit to harvest energy under arm motion. However, they generated very low current output of only 70 and 4 nA for the T-TENG and the PENG, respectively.

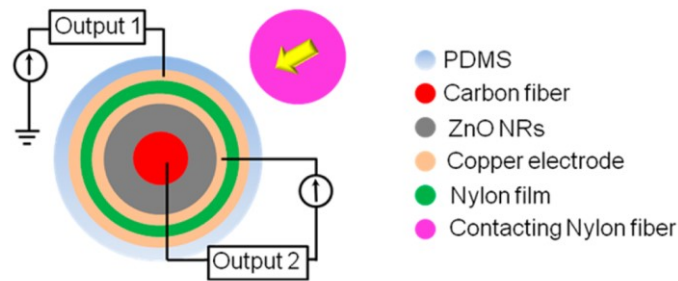


Fig. 15 Schematic illustration of fibre-based hybrid nanogenerator combining a semi-integrated TENG (Output 1) and PENG (Output 2). The power is generated via a contact with an external material (Nylon fibre). Reprinted with permission from Ref. [101]. Copyright 2014 American Chemical Society.

6.2.2. Single-thread fully-integrated T-TENG

Single-thread fully-integrated T-TENG is a stand-alone thread, which is complete with all necessary components of the TENG and can generate electrical power by itself without interaction with any external material. It is typically fabricated in a core-shell structure with one electrode at the core and the other electrode in the shell. The power is produced by relative movement between the core and the shell based on CS-mode and/or LS-mode. As an example, Kim et al. developed a T-TENG from woven fibres. Each fibre comprised a Ag-yarn acting as the core electrode and a flexible tube acting as the shell substrate, as shown in Fig. 16(a) [78]. The outer surface of the tube was coated with AgNWs and a mixture of PDMS and EcoFlex, which served as the other electrode and the insulating layer respectively. The inner surface of

the tube was coated with 1H, 1H, 2H, 2H-perfluorooctyltrichlorosilane (FOTS) to chemically modify the surface by adding fluorine end-functional atoms. This layer increased the output voltage by a factor of 12. The operation principle of the TENG is shown in Fig. 16(b). The contact-separation between the Ag yarn and the FOTS layer under repeated force lead to an alternating current flow between the AgNWs layer and Ag yarn. A 5x5 array of the threads exhibited a power density of 480 mW/m² under a compressive force of 10 N at 3 Hz. Although the size of the thread is fairly large, which is inappropriate for implementing in textiles, it provides a good concept for fibre-based TENG.

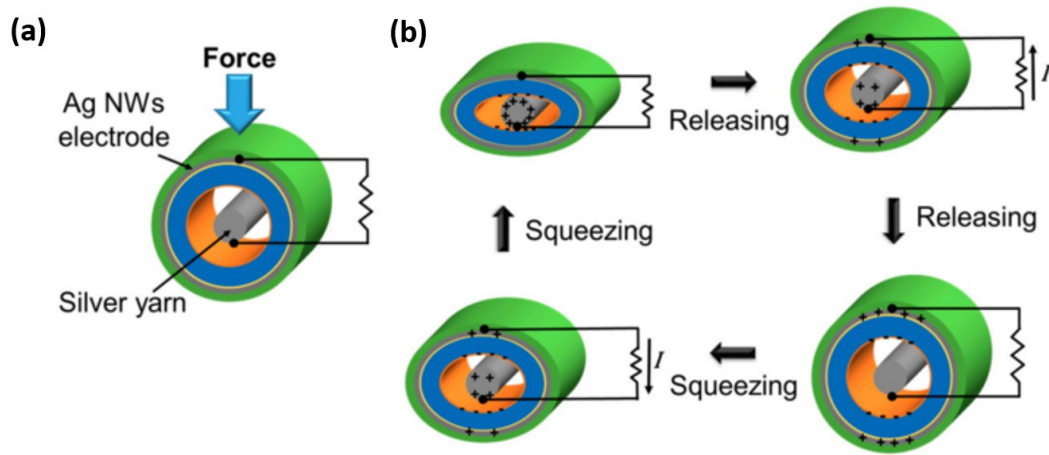


Fig. 16 (a) Schematic illustration of single-thread fully-integrated TENG and (b) its operation principle in CS-mode. Reprinted from Ref. [78]. Copyright 2017 with permission from the authors, MDPI.

Cheng et al. designed a stretchable fibre-based T-TENG also with a core-shell structure [41]. The core fibre comprised a pre-stretched PU fibre coated with AgNWs and PTFE layer. The shell was made from a pre-stretched PDMS film coated with AgNWs. The device could harvest energy from various mechanical energy forms, such as stretching, bending, twisting and pressing. The maximum power of 22.5 $\mu\text{W}/\text{m}^2$ was obtained when the fibre was twisted at a frequency of 1 Hz with a twisting angle of 135° and a load of 50 M Ω . Moreover, the device was demonstrated as a wearable self-powered healthcare monitoring sensors capable of detecting finger bending, walking, breathing, pulse and phonation.

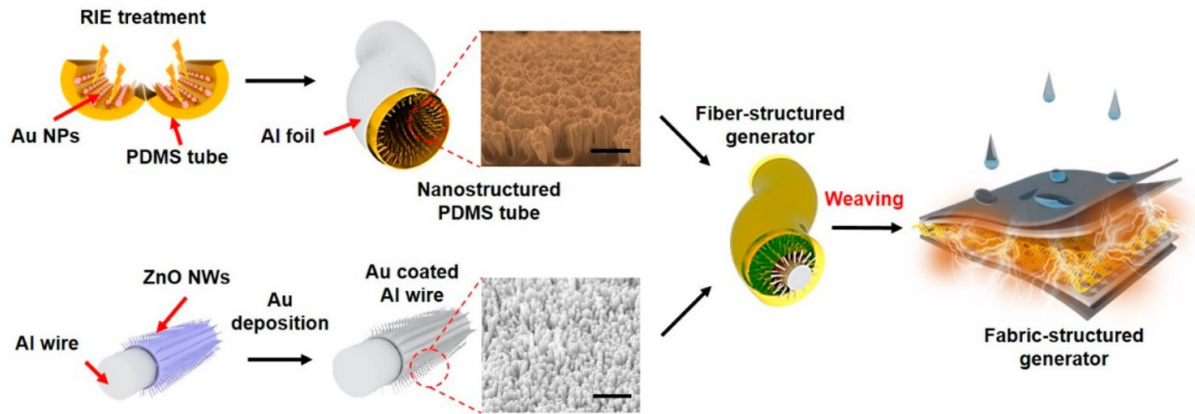


Fig. 17 Schematic diagrams of the fabrication process for the fibre-based TENG revealed by Kim et al. Reprinted with permission from Ref. [39]. Copyright 2015 American Chemical Society.

A surface modified fibre-based T-TENG was revealed by Kim et al. [39] which used nanostructure structures on both the outer surface of the core and the inner surface of the shell (Fig. 17). First, the ZnO NWs were grown on Al wires by a hydrothermal process. Then, it was deposited with thin gold (Au) film using e-beam evaporation. The shell was made from PDMS tube, whose inner wall was etched using RIE forming NWs on the surface. The core was then manually inserted into the PDMS tube and the whole fibre was wrapped in Al foil. Finally, three fibres were assembled together to form weft and warp yarns, which were later woven together to produce a plain fabric. Under a periodic compressive force of 50 N, the T-TENG obtained an instantaneous power density of 204 mW/m^2 , even in a high humidity environment of $\sim 95\% \text{ RH}$.

6.2.3. Multiple-thread fully-integrated T-TENG

Multiple-thread fully-integrated fibre-based T-TENGs require an interaction between at least two fibres to be able to harvest energy. Generally, each fibre will comprise an electrode and the T-TENG will operate in CS-mode, LS-mode or FT-mode. Because of the relative movement between the fibres, the electric potential is built up between the electrodes, as shown in Fig. 18(a). In 2014, the first fibre-based TENG was explored by Zhong et al [20]. It was composed of two modified cotton yarns twisted together. One was a carbon nanotube (CNT)

coated cotton thread (CCT), and the other was a PTFE and CNT coated cotton thread (PCCT). The fabrication process is illustrated in Fig. 18(b). A dipping and drying process was used to produce both the CCTs, where the cotton threads were coated with a MWCNT ink and the PCCTs, where the CCTs were coated with PTFE. Lastly, the CCT and PCCT were entangled together to double-spiral structure and then woven into a fabric. It was employed to harvest energy from finger bending and delivered an average power density of around 1 mW/m^2 . After 90,000 operation cycles, only a minimal decrease in output current was observed, indicating a highly reliable power generator.

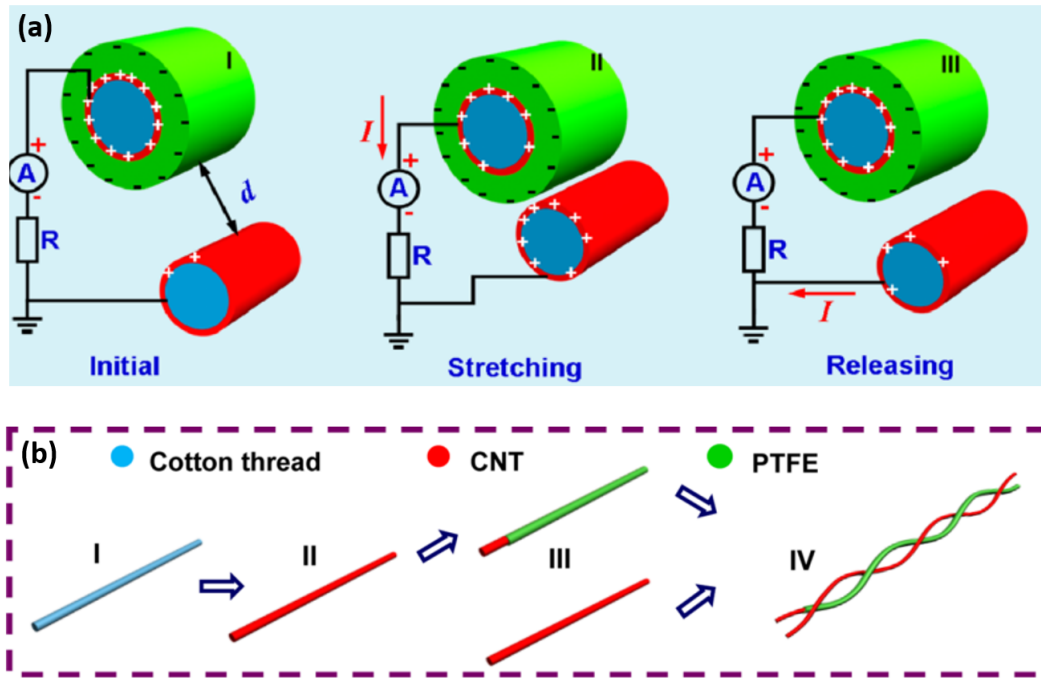


Fig. 18 (a) Power generation mechanism via contact-separation of multiple-thread fully-integrated TENG and (b) schematic illustration of the fabrication process. Reprinted with permission from Ref. [20]. Copyright 2014 American Chemical Society.

Another example of a multiple-thread fully-integrated TENG was presented by Zhao et al., in which all fibres interacted with each other [38]. As shown in Fig. 19 (a), the TENG was constructed by plain-weaving 2-ply Cu-coated PET (Cu-PET) warp yarns and PI-coated Cu-PET (PI-Cu-PET) weft yarns together using an industrial weaving loom. Firstly, 1-ply Cu-PET yarns were prepared by depositing PET yarns using a polymer-assisted metal deposition

method. To decrease the resistance to $0.17 \Omega/\text{cm}$, the 1-ply Cu-PET yarns were spun into the 2-ply Cu-PET yarns. To produce the PI-Cu-PET yarns, the Cu-PET yarns were coated with PI precursor via the dipping and drying method. The properties of the resultant yarns are quite similar to conventional industrial yarns and under cycled deformation, the contact area between weft and warp yarns changed leading to a varying charge distribution at yarn crisscross intersections, shown in Fig. 19(b). The maximum power densities of 23.86 mW/m^2 under bending and 33.16 mW/m^2 under compression were observed. Furthermore, this design exhibited good durability and output power stability even after 1000 tapping cycles and 20 washing cycles.

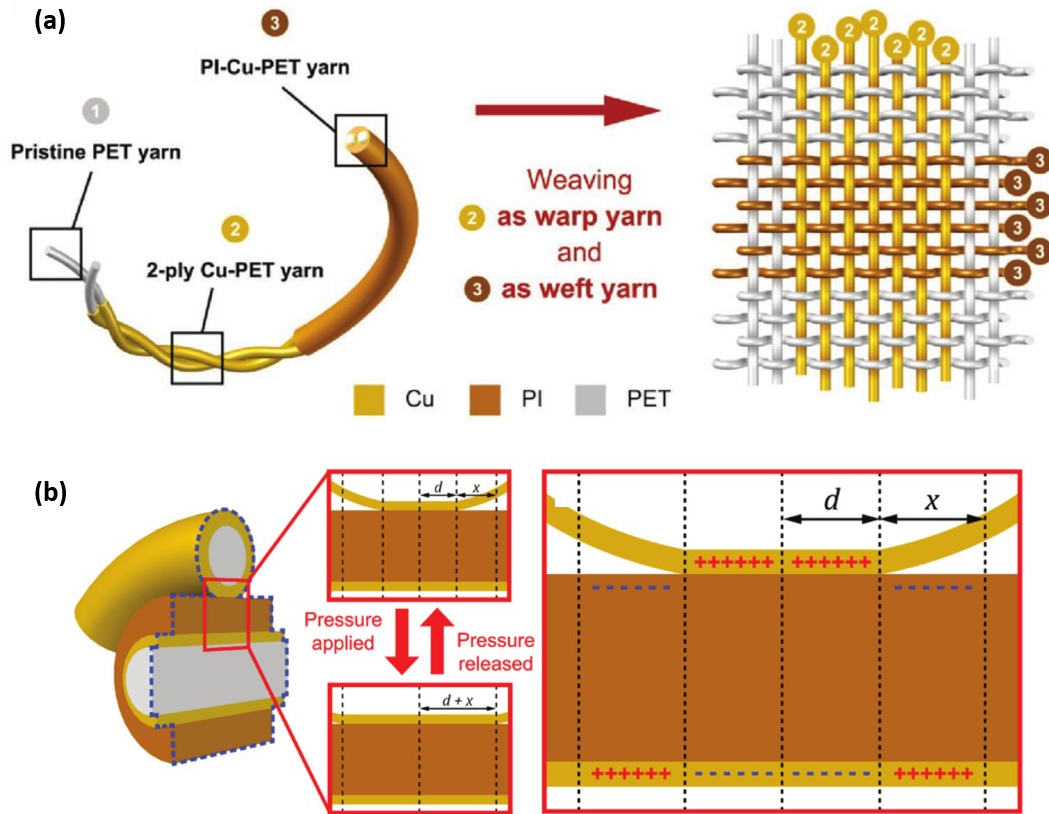


Fig. 19 (a) Schematic illustration of the fabrication process and structure of the T-TENG proposed by Zhao et al. and (b) the working principle of the T-TENG. Reprinted from Ref. [38]. Copyright 2016, with permission from John Wiley & Sons, Inc.

To increase the power output of fibre-based T-TENG, a 3D orthogonal woven TENG was invented by Dong et al [40]. As shown in Fig. 20(a), the generator comprised three stacks of yarns. The middle stack was created from conductive 3-ply-twisted SS/PE fibre blended yarns

(weft yarns). The top and the bottom stacks were made from 3-ply-twisted SS/PE fibre blended yarns (warp yarns) coated with PDMS. The weft and warp yarns were not interlaced, but they were arranged perpendicularly to each other and bound by non-conductive Z-yarns. Under periodic tapping, an AC output was generated between the outer electrodes (top and bottom) and the middle electrodes. Fig. 20(b) and (c) illustrate the frequency dependence of the V_{OC} and I_{SC} , respectively. The V_{OC} rises slightly at low frequency, then remains constant as the frequency increases, whereas the I_{SC} increases considerably with increasing frequency. At a tapping frequency of 3 Hz, a power of 263.36 mW/m² was generated. Moreover, there was no significant decline in the performance after 10 washing cycles and 1500 tapping cycles.

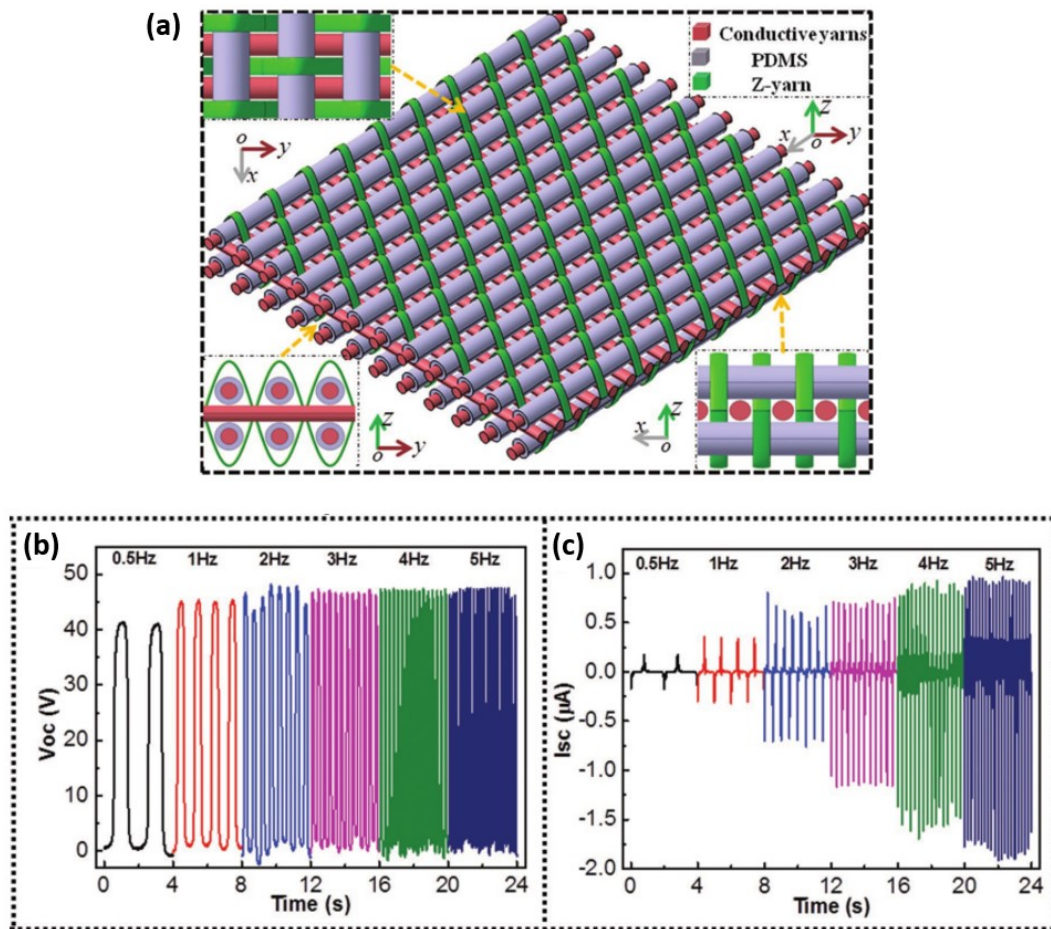


Fig. 20 (a) Schematic illustration of the structure of 3D orthogonal woven TENG. Frequency dependence of (b) V_{OC} and (c) I_{SC} of the TENG. Reprinted from Ref. [40]. Copyright 2017, with permission from John Wiley & Sons, Inc.

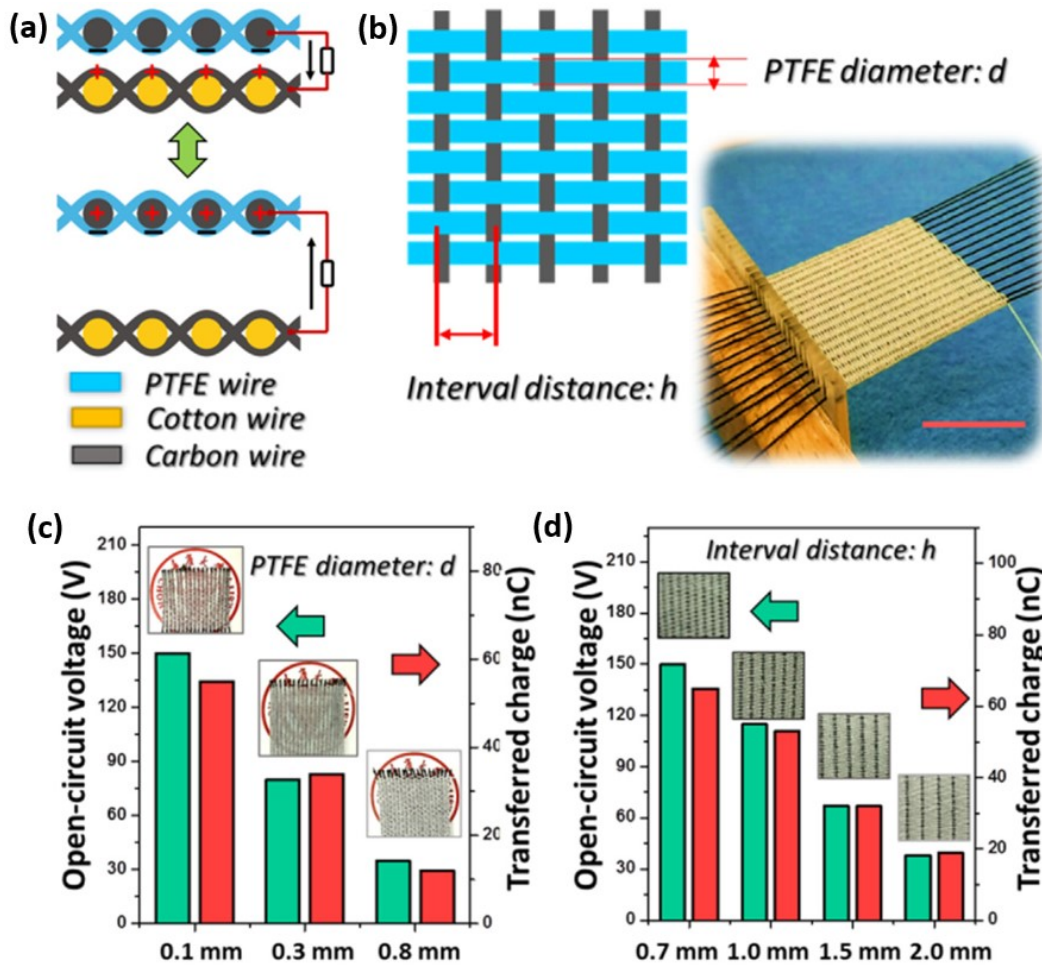


Fig. 21 (a) Power generation mechanism of the T-TENG proposed by Chen et al., (b) Schematic illustration of the woven structure (left side) and photograph (right side) of the T-TENG (scale bar: 2.5 cm), (c) dependence of the V_{OC} and the transferred charges on the PTFE diameter and (d) dependence of the V_{OC} and the transferred charges on the interval distance of the carbon wires. The insets show the photographs of the corresponding T-TENGs. Reprinted from Ref. [102]. Copyright 2018, with permission from Elsevier.

Another T-TENG was demonstrated by Chen et al. who developed a T-TENG by weaving cotton, carbon and PTFE wires on a traditional shuttle-flying weaving machine [102]. In the CS-mode, an alternating current is generated between the carbon wires due to the surface charge caused by the contact between the PTFE wires and the carbon wires, as shown in Fig. 21(a). Furthermore, they have found out that the dimensional features affecting the yarn-packing density, such as the PTFE diameter (d) and the interval distance (h) of the carbon wires (Fig. 21(b)) influence the electrical output of the T-TENG. The results in Fig. 21(c) and (d)

reveal that the V_{OC} and the transferred charge decline with increasing d and h , since an increase in the PTFE diameter results in a reduction in the effective contact area and in the induction effect due to a thicker triboelectric layer. An increase in the interval distance of the carbon wires leads to a decrease in the induced charges. At a frequency of 5 Hz, the T-TENG with $3 \times 3 \text{ cm}^2$ area delivers a V_{OC} of around 175 V and an I_{SC} of around 8 μA .

7. Discussion

Numerous T-TENGs have been demonstrated and are discussed in this review and it is clear triboelectric energy harvesting is well suited to textile-based energy harvesting applications. The various T-TENGs are summarised in Tables 1 and 2, however, it is clear there is a lack of standardisation in the methods and presentation of performance data. In 2015, Zi et al. proposed a structural figure-of-merit, which depends on the operation mode, and a material figure-of-merit, which is the square of the surface charge density [103]. This approach is not widely used because it is difficult to precisely measure the surface charge density. Instead of this, most papers give the electrical outputs of TENG, such as I_{SC} , V_{OC} and quote an area power density. Typically, the values quoted are peak instantaneous values and the duration of the energy generating output is not discussed. There are several examples where TENGs have been used to blink LEDs. In this case, peak outputs are of interest. However, in most cases, the energy harvester output is conditioned and stored for use when the energy is required by the load electronics, which generally require continuous DC power.

Furthermore, these parameters are influenced by various factors, including the humidity, the thickness, the operation frequency, and the contact force, and this detail is often not provided in the literature. For example, the output performance of TENGs is significantly degraded under high humidity condition [39,104,105]. Secondly, TENGs with a larger thickness (e.g. more stacks) deliver a higher area power density [32,33]. Thirdly, a higher

operation frequency leads to a higher power output since I_{SC} increased with frequency, whilst V_{OC} remained constant [40,81,83,100]. Lastly, the output power increases with increasing contact force until it saturates at a certain force, at which point the effective contact area cannot be further increased [33,54,82]. Fig. 22 shows the contact force dependence of the output voltage and current of a T-TENG operating in CS-mode [33]. The output can be divided into three regions: R(i) steep increase region, R(ii) linear increase region and R(iii) saturation region. Another important parameter missing from most papers is the energy conversion efficiency. As mentioned above, it is obvious that with increasing frequency and force, the output power of the TENG rises, since the input power to the system increases. Because of this, it is more expedient to look at the ratio between the input and the output power through the system using Root Mean Square (RMS) values over a given period of time instead of only the instantaneous peak power output. As can be seen in Tables 1 and 2, the papers with a complete set of these parameters can be rarely found. To be able to accurately compare the output performance of TENGs, these parameters have to be considered when performing the experiment and explicitly expressed in the papers.

When comparing the performance of the various T-TENGs given the data available, the peak power density of the fibre-based and the fabric-based devices range from 22.5 nW/m² to 953 mW/m² and from 1.25 to 8,920 mW/m² respectively. The reason why the most fibre-based TENGs tend to produce lower power density compared to the fabric-based TENG could be due to the complexity of the fabrication process. The fabrication of the fabric-based TENGs is less complex and do not require high precision, thus it is easier to perform additional processes, which help improve their output performance. Compared to bulk TENGs with a record power density of 500 W/m² [106], the outputs of T-TENGs are relatively low. One of the main reasons could be a reduction in effective contact area caused by the uneven surface of the textile related to the manufacturing technique used for interlacing the weft and warp yarns. It should be noted

that the previous evaluation excludes a paper that claimed an unusually high power density of 336 W/m^2 [92] at an external load resistance of 20Ω , which is very low compared to other papers with a typical load value in an order of $\text{M}\Omega$. Also, the claimed current density used to calculate the power density is not in good agreement with the output currents, which are only about $78 \mu\text{A}$.

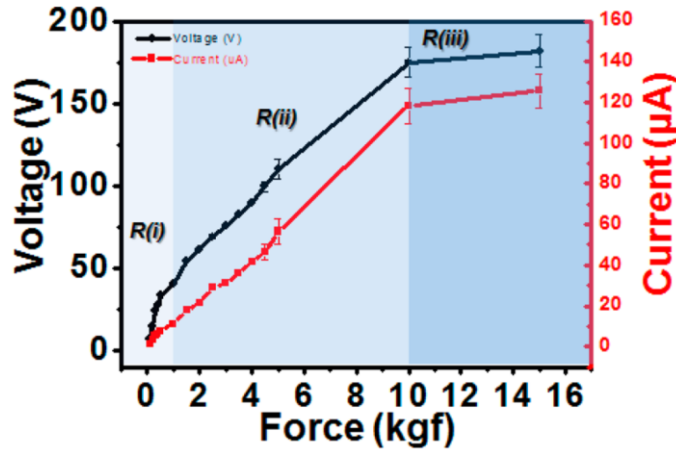


Fig. 22 Contact force dependence of the output voltage and current of the T-TENG operating in CS-mode proposed by Seung et al. Reprinted with permission from Ref. [33]. Copyright 2015 American Chemical Society.

TENGs typically generate a relatively high voltage, which can reach several hundred volts, but very low current in a level of μA . Moreover, the claimed maximum power densities were obtained at the external load resistance in an order of $\text{M}\Omega$. However, in the real application of TENGs, the load resistance of the circuit is much lower and the desired operating voltage is in the range of a few volts. This disparity requires the use of a power conditioning circuit, typically combined with some form of storage. Recently, Xi et al. has proposed a universal power management strategy and achieved an energy conversion efficiency of 85% using a DC buck converter and a power management module [107]. Another power conditioning circuit demonstrated the use of Bennet's doubler circuit, which claims to exponentially boost the output energy of TENGs compared to standard diode bridge circuits [108]. Another approach to reduce this problem is to integrate many small TENGs together to increase the current instead of using a single large size TENG. Concerning the energy storage for T-TENGs, many

research groups have developed textile-based supercapacitor, which can successfully be integrated with the T-TENG [57,100,109] and solve the problem of alternate and unstable power output in the real operation [110]. Given the requirements of practical applications, another method for presenting performance data should be the time taken to charge up a suitable capacitor given a specified mechanical input. This would provide a more complete picture of the energy harvesting potential of a given TENG design and factor in losses at the power conditioning stage. For example, in the case of the TENG shown in Fig. 4 and 5, if the power of the TENG is calculated from the 1- μ F capacitor voltage (Fig. 5(b)), the average power in the capacitor at a saturation voltage of 22.5 V and given a charging time of 170 s is 1.49 μ W. This is significantly lower than the maximum peak power of 22.3 mW at a load resistance of 10 M Ω (Fig. 5(a)).

Due to a wide range of material choices, operating modes and structural designs, T-TENGs have been found in many applications. Most power generation applications involve driving LEDs for lighting, decoration or signalling, such as a wearable night-time warning indicator for pedestrians [49]. T-TENGs have been used to charge a battery [47] or capacitor [100] and power various wearable and portable devices, such as a cell phone [67], calculator, digital watch [79] and wireless systems [51]. For sensing applications, several types of self-powered sensors have been demonstrated, typically in force and strain sensing to monitor motion [40], pressure [101] and personal health [41]. In addition to wearable, there is a clear potential to utilise T-TENGs in other applications that use textiles. For example, to harvest energy from foot traffic using a triboelectric carpet or for self-powered sensing of seat occupancy in car interiors.

Towards a practical implementation of T-TENGs, it is important that the properties of textile remain the same after implementing the T-TENG. Since T-TENGs can be realised using functional yarns, these can be woven or knitted into standard textile structures and have

minimal impact on fabric properties. In the case of fabric-based T-TENGs, thin layers of flexible materials can be used to realize the TENG without affecting the mechanical properties of the textile [111]. Thanks to the nature of textile structures, most T-TENGs are therefore inherently flexible and some of them are stretchable [41,81,99]. One challenge of T-TENGs is that their appearance is often not aesthetically pleasing since the applied coatings will alter the appearance of the fabric. Coatings could potentially reduce breathability depending upon the coating thickness and area affected. Durability and washability are also crucial for T-TENG, since normal clothes should be able to withstand detergents, washing, drying and ironing. Fibre-based T-TENGs have been demonstrated that they can withstand 20 standardised washes [38] or even 120 washes if protected by placing in a laundry bag [56]. However, most papers do not consider washability properly as can be seen in Tables 1 and 2. Additional washing issues include untwisting of yarns, materials abrasion and pilling, shrinkage, wrinkling and drying capability. Given that TENGs operate on frictional contact between two materials, the abrasion of the textile cannot be neglected and standard textile abrasion tests should be performed to quantify device lifetimes. Another approach to avoid abrasion is to design the T-TENGs to operate in the FT-mode, which experience less friction compared to other modes. Finally, the ability to tailor a fabric is highly desirable for the end production of garments, since industrial fabrics are produced in a long roll or material. Yu et al. demonstrated a T-TENG that can be cut in half with each piece retaining almost half of the original output. After sewing them together, the T-TENG returns to nearly full output [56]. This demonstrated T-TENG textiles can in principle be tailored but the electrodes will have to be manually reconnected and that will require extra time and work.

The majority of published work focus on enhancing the performance of T-TENGs and complex and sophisticated fabrication techniques have been demonstrated that are often not suitable for scaling-up and mass production. Many examples of surface modification require

expensive equipment, the size of samples are limited and process are incompatible with roll-to-roll fabrication processes typically associated with textiles. More recently, research has tended to focus on fibre-based TENGs, which can be fabricated in a manner compatible with standard textile manufacturing processes and maintain the properties of a standard yarn. However, this type of T-TENGs exhibit fairly low power outputs. The next-generation of fibre-based T-TENGs will be fully-integrated in the textile and exhibit improved electrical and mechanical properties compared with the current state of the art. Furthermore, the nascent work on T-TENGs co-located in a fabric alongside energy storage devices such as supercapacitor yarns shows great promise for realising textile power modules for multiple applications.

8. Conclusions

This paper has provided a review of Textile-based TENGs (T-TENGs) and has identified that with respect to the structure, T-TENGs can be classified into two main groups, namely fabric-based TENG and fibre-based TENG. Fabrics can be used directly as a triboelectric material but more often they only serve as substrates for other materials that possess better triboelectric properties. The fibre-based TENGs are made of interlacing fibres, which are typically fabricated in a core-shell structure. Most examples of T-TENGs are operated in the vertical contact separate mode (CS-mode) because of the high power output, the simplicity of the fabrication and the nature of human motion, such as footsteps, hand tapping and joint movements that can be coupled to the T-TENG through compressing, stretching or twisting. Concerning the performance of T-TENGs, their power densities are relatively low compared to bulk TENG because of a decrease in their effective contact area relating to their structure. Due to the complexity of the fabrication process, most fibre-based TENGs tend to exhibit lower power density compared to the fabric-based TENGs. The peak power density of the fibre-based and the fabric-based devices vary from 22.5 nW/m² to 953 mW/m² and from 1.25 to 8,920

mW/m², respectively. Apart from performance, the main challenge relating to the implementation of the T-TENG is maintaining the properties of the conventional textile and the use of processes compatible with standard large-scale textile manufacturing. Some processes have been demonstrated that are familiar to the textile industry such as the use of a commercial machine to twist dielectric fibres around conductive fibres resulting in core-shell yarns, which could be afterwards woven or knitted into a fabric. Whilst many novel and interesting textile implementations have been demonstrated with significant peak power outputs, judging the practical power output is not straightforward. This would be aided by the use of RMS values and a discussion around the practical factors that can affect the power output, such as the humidity. Other important parameters are often missing from the literature such as thickness, test frequency and the contact force. The durability of some devices also appears promising with tens of thousands of operating cycles having been demonstrated. Given suitable rigorous characterisation of performance and lifetime, T-TENGs may well offer a practical approach for energy harvesting for textile-based applications.

Table 1 Summary of important parameters of fabric-based TENGs

Mode	Triboelectric material	Electrode	Substrate	Surface modification	Area (cm ²)	Frequency (Hz)	Force (N)	Voltage (V)	Current (μA)	Power density (mW/m ²)	Durability Test (cycles)	Washability Test (times)	Refs
FCS	Nylon, PE and acrylic	Ag	-	-	125.4	-	-	95	2.5	-	-	-	[22]
CS	Nylon and PTFE	MWCNT, PEDOT:PSS And CF	-	-	17.35	-	-	109.6	0.35	8	-	-	[34]
LS	Nylon and Dacron	Cu foil	Cotton	-	588	43(Grating)	30	2000	200	-	5,400	Washable	[47]
SE	Nylon and FEP	Ag	Nylon	-	16	5	-	22	2	46.5	24,000	Washable	[49]
SE	Fabrics and PDMS	CNT	Cotton	-	16	8	-	200	0.6	37.5	170,000	-	[51]
SE	Al, fabrics and PDMS	Al	-	FOTS-SAM	6	1.25	3	105	27	1,800	20,000	-	[52]
SE	PDMS and fabrics	Graphene	PET	NWs and Plasma treatments	9	-	72	47.1	7	144	-	-	[82]
CS	Nylon and PTFE	Graphene	Nylon	-	3	1	-	3.5	0.28	53.3	-	-	[83]
CS	Nylon and elastomer	Ag	PET	Cu NPs	16	-	60	470	26	7500	3000	-	[93]
CS	Silk and SR	Sn/Cu/Ag	Nylon	-	15	4	2	28.13	2.71	166	-	-	[99]
LS, CS	PU/AL and PI/PDMS	Carbon	Fabric	-	45	1.5	2	33	0.25	1.8	-	-	[21]
CS, FCS,LS	Ni and parylene	Ni	PE	-	25	0.7	-	50	4	393.7	-	Washable	[23]
CS	CF and PVDF	CF	Fabric	Nano-structured	30	1.8	-	210	45	700	-	-	[29]
CS	PET and PDMS	Ag and CNT	PET	Pyramids	25	1	400	500	20	153.8	3,000	-	[30]
CS	PET and FAS	Al foil and AgNW	Nylon	-	9	1.8	-	575	12.1	2,770	12,000	-	[31]
CS	Ni and PDMS	Ni	PET	-	6.25	0.5	35-40	23.39	0.39	1.25	-	-	[32]
CS	Ag and PDMS	Ag	Fabric	ZnO NWs	-	-	100	170	120	-	12,000	-	[33]
FT	Ni/Parylene	Ni	PE	-	22	500(Grating)	-	105	55	3200	1200	Washable	[55]
FCS	Ni and SR	Ni	PE	-	25	3	300	540	140	8,920	100,000	-	[58]
CS	Silk and PVDF	CF	Fabric	Nanofibre	8	2	25.7	500	12	3100	10000	-	[65]

CS	PU and PDMS	CF and carbon-based PU	Fabric	-	133	1.6	760	1468 RMS(566)	25.4 RMS(5.9)	356.6 RMS(135.1)	-	-	[70]
SE	Al NPs and PDMS	AlNPs	Fabric	NPs, NWs	49	1.2	-	250	78	336,000	-	-	[92]
SE	PTFE and CNT	CNT	Cotton	-	20	7	-	100	2	121	10,000	5	[109]

Table 2 Summary of important parameters of fibre-based TENGs

Mode	Triboelectric material	Electrode	Substrate	Surface modification	Area (cm ²)	Frequency (Hz)	Force (N)	Voltage (V)	Current (μA)	Power density (mW/m ²)	Durability Test (cycles)	Washability Test (times)	Refs
CS	Ag and PVDF-TrFE	Ag	PU	-	-	10	-	0.024	-	-	10,000	-	[36]
SE	Skin and SR	SS	fabric	-	146.7	-	-	200	200	953	-	-	[54]
SE, CS, FT	PU and PE	SS	-	-	36	-	-	75	1.2	60	5 h, 8 cm/s	120	[56]
CS	ZnO and PDMS	SS	-	NWs and NPs	2.52	-	-	140.4	21.54	1.2	1,000	-	[97]
SE	Acrylic and SR	SS	-	-	16	3	11	150	0.96	85	50,000	15	[100]
SE	Nylon and PDMS	Cu	Carbon fibre	-	1.08	2	-	23	0.3	42.6	-	-	[101]
CS	Au and PDMS	Al wire and Al foil	-	NWs	196	10	50	40	210	204	-	-	[39]
CS	AgNWs and PTFE	Ag NW	PDMS and PU	AgNWs	-	1	0.05	0.66	0.02	0.0225	4,000	-	[41]
CS	Nylon and SR	Metal wire	PDMS	-	-	0.5	-	4	0.08	1.3	1,600	-	[42]
CS	Ni and SR	Ni and CNTs	SR	-	18.85	3	300	380	11	869	21600	-	[69]
CS	Ag and SR	AgNWs and Ag yarn	-	FOTS	36	3	10	37	36	480	8,000	-	[78]
CS	Cu and SR	Cu and CNT	-	-	-	2	-	142.8	7.38	15	10,800	-	[81]
CS	CNT and PTFE	CNT	Cotton	-	-	5	-	-	0.01122	1	90,000	-	[20]
CS	Cu and PI	Cu	PET	-	24	10 cm/s	-	4.98	37.2	33.16	1,000	20	[38]
CS	SS and PDMS	SS	PE	-	18	3	-	45	9.9	263.36	1,500	10	[40]
CS	Ag and PTFE	Ag	-	-	100	3.3	-	RMS(23.5)	RMS(1.05)	RMS(6)	-	-	[66]
CS	Cu and PTFE	Cu	-	-	16	-	-	18	0.9	-	-	-	[67]
CS, FT	Carbon and PTFE	Carbon	Cotton	-	9	5	-	175	8	-	36000	-	[102]

Acknowledgements

The authors gratefully acknowledge the Engineering and Physical Sciences Research Council (EPSRC) for supporting this research with grant reference EP/P010164/1.

References

- [1] Y. Qi, M.C. McAlpine, Nanotechnology-enabled flexible and biocompatible energy harvesting, *Energy Environ. Sci.* 3 (2010) 1275. doi:10.1039/c0ee00137f.
- [2] Three dimensional photovoltaic fibers for wearable energy harvesting and conversion.pdf, (n.d.).
- [3] J. Liu, Y. Li, S. Arumugam, J. Tudor, S. Beeby, Screen Printed Dye-Sensitized Solar Cells (DSSCs) on Woven Polyester Cotton Fabric for Wearable Energy Harvesting Applications, *Mater. Today Proc.* 5 (2018) 13753–13758. doi:10.1016/j.matpr.2018.02.015.
- [4] R. Mather, J. Wilson, Fabrication of Photovoltaic Textiles, *Coatings.* 7 (2017) 63. doi:10.3390/coatings7050063.
- [5] Q. Wu, J. Hu, A novel design of wearable thermoelectric generator based on 3D fabric structure, *Smart Mater. Struct.*, at press (2017). <https://doi.org/10.1088/1361-665X/aa5694>.
- [6] Z. Cao, M.J. Tudor, R.N. Torah, S.P. Beeby, Screen Printable Flexible BiTe-SbTe-Based Composite Thermoelectric Materials on Textiles for Wearable Applications, *IEEE Trans. Electron Devices.* 63 (2016) 4024–4030. doi:10.1109/TED.2016.2603071.
- [7] J.A. Lee, A.E. Aliev, J.S. Bykova, M.J. de Andrade, D. Kim, H.J. Sim, X. Lepró, A.A. Zakhidov, J.B. Lee, G.M. Spinks, S. Roth, S.J. Kim, R.H. Baughman, Woven-Yarn Thermoelectric Textiles, *Adv. Mater.* (2016) 5038–5044. doi:10.1002/adma.201600709.
- [8] S. Song, K.S. Yun, Design and characterization of scalable woven piezoelectric energy harvester for wearable applications, *Smart Mater. Struct.* 24 (2015). doi:10.1088/0964-1726/24/4/045008.
- [9] D. Matsouka, S. Vassiliadis, D.V. Bayramol, Piezoelectric textile fibres for wearable energy harvesting systems, *Mater. Res. Express.* 5 (2018) 0–10. doi:10.1088/2053-1591/aac928.
- [10] A. Almusallam, Z. Luo, A. Komolafe, K. Yang, A. Robinson, R. Torah, S. Beeby, Flexible piezoelectric nano-composite films for kinetic energy harvesting from textiles, *Nano Energy.* 33 (2017) 146–156. doi:10.1016/j.nanoen.2017.01.037.
- [11] F.-R. Fan, Z.-Q. Tian, Z. Lin Wang, Flexible triboelectric generator, *Nano Energy.* 1 (2012) 328–334. doi:10.1016/j.nanoen.2012.01.004.
- [12] Y. Yang, G. Zhu, H. Zhang, J. Chen, X. Zhong, Z.H. Lin, Y. Su, P. Bai, X. Wen, Z.L. Wang, Triboelectric nanogenerator for harvesting wind energy and as self-powered wind vector sensor system, *ACS Nano.* 7 (2013) 9461–9468. doi:10.1021/nn4043157.
- [13] L. Zhang, B. Zhang, J. Chen, L. Jin, W. Deng, J. Tang, H. Zhang, H. Pan, M. Zhu, W. Yang, Z.L. Wang, Lawn Structured Triboelectric Nanogenerators for Scavenging Sweeping Wind Energy on Rooftops, *Adv. Mater.* 28 (2016) 1650–1656. doi:10.1002/adma.201504462.
- [14] B. Dudem, D.H. Kim, J.S. Yu, Triboelectric nanogenerators with gold-thin-film-coated conductive textile as floating electrode for scavenging wind energy, *Nano Res.* 11 (2017) 1–13. doi:10.1007/s12274-017-1609-0.
- [15] T. Jiang, L.M. Zhang, X. Chen, C.B. Han, W. Tang, C. Zhang, L. Xu, Z.L. Wang, Structural Optimization of Triboelectric Nanogenerator for Harvesting Water Wave Energy, *ACS Nano.* 9 (2015) 12562–12572. doi:10.1021/acsnano.5b06372.
- [16] T. Jiang, Y. Yao, L. Xu, L. Zhang, T. Xiao, Z.L. Wang, Spring-assisted triboelectric nanogenerator for efficiently harvesting water wave energy, *Nano Energy.* 31 (2017) 560–567. doi:10.1016/j.nanoen.2016.12.004.
- [17] T.C. Hou, Y. Yang, H. Zhang, J. Chen, L.J. Chen, Z. Lin Wang, Triboelectric nanogenerator built inside shoe insole for harvesting walking energy, *Nano Energy.* 2 (2013) 856–862. doi:10.1016/j.nanoen.2013.03.001.
- [18] M. Ha, J. Park, Y. Lee, H. Ko, Triboelectric generators and sensors for self-powered wearable electronics, *ACS Nano.* 9 (2015) 3421–3427. doi:10.1021/acsnano.5b01478.

- [19] A. Proto, M. Penhaker, S. Conforto, M. Schmid, Nanogenerators for Human Body Energy Harvesting, *Trends Biotechnol.* 35 (2017) 610–624. doi:10.1016/j.tibtech.2017.04.005.
- [20] J. Zhong, Y. Zhang, Q. Zhong, Q. Hu, B. Hu, Z.L. Wang, J. Zhou, Fiber-Based Generator for Wearable Electronics and Mobile Medication, *ACS Nano.* 8 (2014) 6273–6280. doi:10.1021/nn501732z.
- [21] S. Jung, J. Lee, T. Hyeon, M. Lee, D.H. Kim, Fabric-based integrated energy devices for wearable activity monitors, *Adv. Mater.* 26 (2014) 6329–6334. doi:10.1002/adma.201402439.
- [22] T. Zhou, C. Zhang, C.B. Han, F.R. Fan, W. Tang, Z.L. Wang, Woven structured triboelectric nanogenerator for wearable devices, *ACS Appl. Mater. Interfaces.* 6 (2014) 14695–14701. doi:10.1021/am504110u.
- [23] X. Pu, L. Li, H. Song, C. Du, Z. Zhao, C. Jiang, G. Cao, W. Hu, Z.L. Wang, A self-charging power unit by integration of a textile triboelectric nanogenerator and a flexible lithium-ion battery for wearable electronics, *Adv. Mater.* 27 (2015) 2472–2478. doi:10.1002/adma.201500311.
- [24] Z. Lin, J. Yang, X. Li, Y. Wu, W. Wei, J. Liu, J. Chen, J. Yang, Large-Scale and Washable Smart Textiles Based on Triboelectric Nanogenerator Arrays for Self-Powered Sleeping Monitoring, *Adv. Funct. Mater.* 28 (2018) 1704112. doi:10.1002/adfm.201704112.
- [25] Z. Zhao, X. Pu, C. Du, L. Li, C. Jiang, W. Hu, Z.L. Wang, Freestanding Flag-Type Triboelectric Nanogenerator for Harvesting High-Altitude Wind Energy from Arbitrary Directions, *ACS Nano.* 10 (2016) 1780–1787. doi:10.1021/acsnano.5b07157.
- [26] Z.L. Wang, J. Chen, L. Lin, Progress in triboelectric nanogenerators as a new energy technology and self-powered sensors, *Energy Environ. Sci.* 8 (2015) 2250–2282. doi:10.1039/C5EE01532D.
- [27] Q. Zheng, B. Shi, Z. Li, Z.L. Wang, Recent Progress on Piezoelectric and Triboelectric Energy Harvesters in Biomedical Systems, *Adv. Sci.* 4 (2017) 1700029. doi:10.1002/advs.201700029.
- [28] S. Wang, L. Lin, Z.L. Wang, Triboelectric nanogenerators as self-powered active sensors, *Nano Energy.* 11 (2015) 436–462. doi:10.1016/j.nanoen.2014.10.034.
- [29] T. Huang, C. Wang, H. Yu, H. Wang, Q. Zhang, M. Zhu, Human walking-driven wearable all-fiber triboelectric nanogenerator containing electrospun polyvinylidene fluoride piezoelectric nanofibers, *Nano Energy.* 14 (2015) 226–235. doi:10.1016/j.nanoen.2015.01.038.
- [30] L. Liu, J. Pan, P. Chen, J. Zhang, X. Yu, X. Ding, B. Wang, X. Sun, H. Peng, A triboelectric textile templated by a three-dimensionally penetrated fabric, *J. Mater. Chem. A.* 4 (2016) 6077–6083. doi:10.1039/C6TA01166G.
- [31] Y. Guo, K. Li, C. Hou, Y. Li, Q. Zhang, H. Wang, Fluoroalkylsilane-Modified Textile-Based Personal Energy Management Device for Multifunctional Wearable Applications, *ACS Appl. Mater. Interfaces.* 8 (2016) 4676–4683. doi:10.1021/acsami.5b11622.
- [32] Y.H. Ko, G. Nagaraju, J.S. Yu, Multi-stacked PDMS-based triboelectric generators with conductive textile for efficient energy harvesting, *RSC Adv.* 5 (2015) 6437–6442. doi:10.1039/c4ra15310c.
- [33] W. Seung, M.K. Gupta, K.Y. Lee, K. Shin, J. Lee, T.Y. Kim, S. Kim, J. Lin, J.H. Kim, S. Kim, Nanopatterned Textile-Based Wearable Triboelectric Nanogenerator, *ACS Nano.* 9 (2015) 3501–3509. doi:10.1021/nn507221f.
- [34] P.S. Das, J.Y. Park, D.H. Kim, Vacuum filtered conductive nylon membrane-based flexible TENG for wearable electronics, *Micro Nano Lett.* 12 (2017) 697–700. doi:10.1049/mnl.2017.0170.
- [35] C. Wu, T.W. Kim, F. Li, T. Guo, Wearable Electricity Generators Fabricated Utilizing Transparent Electronic Textiles Based on Polyester/Ag Nanowires/Graphene Core-Shell Nanocomposites, *ACS Nano.* 10 (2016) 6449–6457. doi:10.1021/acsnano.5b08137.
- [36] H.J. Sim, C. Choi, S.H. Kim, K.M. Kim, C.J. Lee, Y.T. Kim, X. Lepró, R.H. Baughman, S.J. Kim, Stretchable Triboelectric Fiber for Self-powered Kinematic Sensing Textile, *Sci. Rep.* 6 (2016) 35153. doi:10.1038/srep35153.
- [37] Z. Wen, M.-H. Yeh, H. Guo, J. Wang, Y. Zi, W. Xu, J. Deng, L. Zhu, X. Wang, C. Hu, L. Zhu, X. Sun, Z.L. Wang, Self-powered textile for wearable electronics by hybridizing fiber-shaped nanogenerators, solar cells, and supercapacitors, *Sci. Adv.* 2 (2016) e1600097–e1600097. doi:10.1126/sciadv.1600097.
- [38] Z. Zhao, C. Yan, Z. Liu, X. Fu, L.-M. Peng, Y. Hu, Z. Zheng, Machine-Washable Textile Triboelectric Nanogenerators for Effective Human Respiratory Monitoring through Loom Weaving of Metallic Yarns, *Adv. Mater.* 28 (2016) 10267–10274. doi:10.1002/adma.201603679.
- [39] K.N. Kim, J. Chun, J.W. Kim, K.Y. Lee, J.-U. Park, S.-W. Kim, Z.L. Wang, J.M. Baik, Highly Stretchable 2D Fabrics for Wearable Triboelectric Nanogenerator under Harsh Environments, *ACS Nano.* 9 (2015) 6394–6400. doi:10.1021/acsnano.5b02010.

- [40] K. Dong, J. Deng, Y. Zi, Y.-C. Wang, C. Xu, H. Zou, W. Ding, Y. Dai, B. Gu, B. Sun, Z.L. Wang, 3D Orthogonal Woven Triboelectric Nanogenerator for Effective Biomechanical Energy Harvesting and as Self-Powered Active Motion Sensors, *Adv. Mater.* 29 (2017) 1702648. doi:10.1002/adma.201702648.
- [41] Y. Cheng, X. Lu, K. Hoe Chan, R. Wang, Z. Cao, J. Sun, G. Wei Ho, A stretchable fiber nanogenerator for versatile mechanical energy harvesting and self-powered full-range personal healthcare monitoring, *Nano Energy*. 41 (2017) 511–518. doi:10.1016/j.nanoen.2017.10.010.
- [42] W. Gong, C. Hou, Y. Guo, J. Zhou, J. Mu, Y. Li, Q. Zhang, H. Wang, A wearable, fibroid, self-powered active kinematic sensor based on stretchable sheath-core structural triboelectric fibers, *Nano Energy*. 39 (2017) 673–683. doi:10.1016/j.nanoen.2017.08.003.
- [43] S. Wang, L. Lin, Y. Xie, Q. Jing, S. Niu, Z.L. Wang, Sliding-triboelectric nanogenerators based on in-plane charge-separation mechanism, *Nano Lett.* 13 (2013) 2226–2233. doi:10.1021/nl400738p.
- [44] L. Lin, S. Wang, Y. Xie, Q. Jing, S. Niu, Y. Hu, Z.L. Wang, Segmentally structured disk triboelectric nanogenerator for harvesting rotational mechanical energy, *Nano Lett.* 13 (2013) 2916–2923. doi:10.1021/nl4013002.
- [45] P. Bai, G. Zhu, Y. Liu, J. Chen, Q. Jing, W. Yang, J. Ma, G. Zhang, Z.L. Wang, Cylindrical Rotating Triboelectric Nanogenerator, *ACS Nano*. 7 (2013) 6361–6366. doi:10.1021/nn402491y.
- [46] S. Niu, S. Wang, Y. Liu, Y.S. Zhou, L. Lin, Y. Hu, K.C. Pradel, Z.L. Wang, A theoretical study of grating structured triboelectric nanogenerators, *Energy Environ. Sci.* 7 (2014) 2339–2349. doi:10.1039/c4ee00498a.
- [47] N. Cui, J. Liu, L. Gu, S. Bai, X. Chen, Y. Qin, Wearable Triboelectric Generator for Powering the Portable Electronic Devices, *ACS Appl. Mater. Interfaces*. 7 (2015) 18225–18230. doi:10.1021/am5071688.
- [48] S. Niu, Y. Liu, S. Wang, L. Lin, Y.S. Zhou, Y. Hu, Z.L. Wang, Theoretical Investigation and Structural Optimization of Single-Electrode Triboelectric Nanogenerators, *Adv. Funct. Mater.* 24 (2014) 3332–3340. doi:10.1002/adfm.201303799.
- [49] S. Li, Q. Zhong, J. Zhong, X. Cheng, B. Wang, B. Hu, J. Zhou, Cloth-based power shirt for wearable energy harvesting and clothes ornamentation, *ACS Appl. Mater. Interfaces*. 7 (2015) 14912–14916. doi:10.1021/acsami.5b03680.
- [50] M. Shi, J. Zhang, M. Han, Y. Song, Z. Su, H. Zhang, A single-electrode wearable triboelectric nanogenerator based on conductive & stretchable fabric, in: 2016 IEEE 29th Int. Conf. Micro Electro Mech. Syst., IEEE, 2016: pp. 1228–1231. doi:10.1109/MEMSYS.2016.7421859.
- [51] M. Shi, H. Wu, J. Zhang, M. Han, B. Meng, H. Zhang, Self-powered wireless smart patch for healthcare monitoring, *Nano Energy*. 32 (2017) 479–487. doi:10.1016/j.nanoen.2017.01.008.
- [52] G. Song, Y. Kim, S. Yu, M.O. Kim, S.H. Park, S.M. Cho, D.B. Velusamy, S.H. Cho, K.L. Kim, J. Kim, E. Kim, C. Park, Molecularly Engineered Surface Triboelectric Nanogenerator by Self-Assembled Monolayers (METS), *Chem. Mater.* 27 (2015) 4749–4755. doi:10.1021/acs.chemmater.5b01507.
- [53] Q. Zhang, Q. Liang, Q. Liao, F. Yi, X. Zheng, M. Ma, F. Gao, Y. Zhang, Service Behavior of Multifunctional Triboelectric Nanogenerators, *Adv. Mater.* 29 (2017) 1606703. doi:10.1002/adma.201606703.
- [54] Y.-C. Lai, J. Deng, S.L. Zhang, S. Niu, H. Guo, Z.L. Wang, Single-Thread-Based Wearable and Highly Stretchable Triboelectric Nanogenerators and Their Applications in Cloth-Based Self-Powered Human-Interactive and Biomedical Sensing, *Adv. Funct. Mater.* 27 (2017) 1604462. doi:10.1002/adfm.201604462.
- [55] X. Pu, W. Song, M. Liu, C. Sun, C. Du, C. Jiang, X. Huang, D. Zou, W. Hu, Z.L. Wang, Wearable Power-Textiles by Integrating Fabric Triboelectric Nanogenerators and Fiber-Shaped Dye-Sensitized Solar Cells, *Adv. Energy Mater.* 6 (2016) 1601048. doi:10.1002/aenm.201601048.
- [56] A. Yu, X. Pu, R. Wen, M. Liu, T. Zhou, K. Zhang, Y. Zhang, J. Zhai, W. Hu, Z.L. Wang, Core–Shell-Yarn-Based Triboelectric Nanogenerator Textiles as Power Cloths, *ACS Nano*. 11 (2017) 12764–12771. doi:10.1021/acsnano.7b07534.
- [57] X. Pu, L. Li, M. Liu, C. Jiang, C. Du, Z. Zhao, W. Hu, Z.L. Wang, Wearable Self-Charging Power Textile Based on Flexible Yarn Supercapacitors and Fabric Nanogenerators, *Adv. Mater.* 28 (2016) 98–105. doi:10.1002/adma.201504403.
- [58] Z. Tian, J. He, X. Chen, Z. Zhang, T. Wen, C. Zhai, J. Han, J. Mu, X. Hou, X. Chou, C. Xue, Performance-boosted triboelectric textile for harvesting human motion energy, *Nano Energy*. 39 (2017) 562–570. doi:10.1016/j.nanoen.2017.06.018.
- [59] R. Kamiya, B.A. Cheeseman, P. Popper, T.-W. Chou, Some recent advances in the fabrication and design of three-dimensional textile preforms: a review, *Compos. Sci. Technol.* 60 (2000) 33–47. doi:10.1016/S0266-

- [60] W.E. Morton, J.W.S. Hearle, Physical properties of textile fibres, fourth ed., Woodhead Publishing Limited, Cambridge, 2008. doi:10.1533/9781845694425.
- [61] B.P. Corbman, Textiles : Fiber to Fabric, sixth ed., Gregg Division/McGraw-Hill Book Company, New York, 1983.
- [62] K. Bilisik, N.S. Karaduman, N.E. Bilisik, 3D Fabrics for Technical Textile Applications, in: Non-Woven Fabr., InTech, 2016. doi:10.5772/61224.
- [63] J. Peterson, Customisation of Fashion Products Using Complete Garment Technology, 2012.
- [64] N. Bhardwaj, S.C. Kundu, Electrospinning: A fascinating fiber fabrication technique, Biotechnol. Adv. 28 (2010) 325–347. doi:10.1016/j.biotechadv.2010.01.004.
- [65] Y. Guo, X.S. Zhang, Y. Wang, W. Gong, Q. Zhang, H. Wang, J. Brugger, All-fiber hybrid piezoelectric-enhanced triboelectric nanogenerator for wearable gesture monitoring, Nano Energy. 48 (2018) 152–160. doi:10.1016/j.nanoen.2018.03.033.
- [66] S.S. Kwak, H. Kim, W. Seung, J. Kim, R. Hinchet, S.-W. Kim, Fully Stretchable Textile Triboelectric Nanogenerator with Knitted Fabric Structures, ACS Nano. 11 (2017) 10733–10741. doi:10.1021/acsnano.7b05203.
- [67] J. Chen, Y. Huang, N. Zhang, H. Zou, R. Liu, C. Tao, X. Fan, Z.L. Wang, Micro-cable structured textile for simultaneously harvesting solar and mechanical energy, Nat. Energy. 1 (2016) 16138. doi:10.1038/nenergy.2016.138.
- [68] J.W. Lee, B.U. Ye, J.M. Baik, Research Update: Recent progress in the development of effective dielectrics for high-output triboelectric nanogenerator, APL Mater. 5 (2017). doi:10.1063/1.4979306.
- [69] Z. Tian, J. He, X. Chen, T. Wen, C. Zhai, Z. Zhang, J. Cho, X. Chou, C. Xue, Core-shell coaxially structured triboelectric nanogenerator for energy harvesting and motion sensing, RSC Adv. 8 (2018) 2950–2957. doi:10.1039/C7RA12739A.
- [70] R.I. Haque, P.-A. Farine, D. Briand, Soft triboelectric generators by use of cost-effective elastomers and simple casting process, Sensors Actuators A Phys. 271 (2018) 88–95. doi:10.1016/j.sna.2017.12.018.
- [71] S. Niu, S. Wang, L. Lin, Y. Liu, Y.S. Zhou, Y. Hu, Z.L. Wang, Theoretical study of contact-mode triboelectric nanogenerators as an effective power source, Energy Environ. Sci. 6 (2013) 3576. doi:10.1039/c3ee42571a.
- [72] S. Niu, Y. Liu, S. Wang, L. Lin, Y.S. Zhou, Y. Hu, Z.L. Wang, Theory of sliding-mode triboelectric nanogenerators, Adv. Mater. 25 (2013) 6184–6193. doi:10.1002/adma.201302808.
- [73] V. Kaushik, J. Lee, J. Hong, S. Lee, S. Lee, J. Seo, C. Mahata, T. Lee, Textile-Based Electronic Components for Energy Applications: Principles, Problems, and Perspective, Nanomaterials. 5 (2015) 1493–1531. doi:10.3390/nano5031493.
- [74] J. Lee, H. Kwon, J. Seo, S. Shin, J.H. Koo, C. Pang, S. Son, J.H. Kim, Y.H. Jang, D.E. Kim, T. Lee, Conductive fiber-based ultrasensitive textile pressure sensor for wearable electronics, Adv. Mater. 27 (2015) 2433–2439. doi:10.1002/adma.201500009.
- [75] R.B. Reed, T. Zaikova, A. Barber, M. Simonich, R. Lankone, M. Marco, K. Hristovski, P. Herckes, L. Passantino, D.H. Fairbrother, R. Tanguay, J.F. Ranville, J.E. Hutchison, P.K. Westerhoff, Potential Environmental Impacts and Antimicrobial Efficacy of Silver- and Nanosilver-Containing Textiles, Environ. Sci. Technol. 50 (2016) 4018–4026. doi:10.1021/acs.est.5b06043.
- [76] X. Wang, H. Hu, Y. Shen, X. Zhou, Z. Zheng, Stretchable conductors with ultrahigh tensile strain and stable metallic conductance enabled by prestrained polyelectrolyte nanoplateforms, Adv. Mater. 23 (2011) 3090–3094. doi:10.1002/adma.201101120.
- [77] F. Xu, Y. Zhu, Highly conductive and stretchable silver nanowire conductors, Adv. Mater. 24 (2012) 5117–5122. doi:10.1002/adma.201201886.
- [78] K. Kim, G. Song, C. Park, K.S. Yun, Multifunctional woven structure operating as triboelectric energy harvester, capacitive tactile sensor array, and piezoresistive strain sensor array, Sensors (Switzerland). 17 (2017). doi:10.3390/s17112582.
- [79] Y. Yang, N. Sun, Z. Wen, P. Cheng, H. Zheng, H. Shao, Y. Xia, C. Chen, H. Lan, X. Xie, C. Zhou, J. Zhong, X. Sun, S.T. Lee, Liquid-Metal-Based Super-Stretchable and Structure-Designable Triboelectric Nanogenerator for Wearable Electronics, ACS Nano. 12 (2018) 2027–2034. doi:10.1021/acsnano.8b00147.
- [80] W. Zeng, L. Shu, Q. Li, S. Chen, F. Wang, X.M. Tao, Fiber-based wearable electronics: A review of materials, fabrication, devices, and applications, Adv. Mater. 26 (2014) 5310–5336. doi:10.1002/adma.201400633.

- [81] X. He, Y. Zi, H. Guo, H. Zheng, Y. Xi, C. Wu, J. Wang, W. Zhang, C. Lu, Z.L. Wang, A Highly Stretchable Fiber-Based Triboelectric Nanogenerator for Self-Powered Wearable Electronics, *Adv. Funct. Mater.* 27 (2017) 1604378. doi:10.1002/adfm.201604378.
- [82] H. Chu, H. Jang, Y. Lee, Y. Chae, J.-H. Ahn, Conformal, graphene-based triboelectric nanogenerator for self-powered wearable electronics, *Nano Energy*. 27 (2016) 298–305. doi:10.1016/j.nanoen.2016.07.009.
- [83] M. Zhu, Y. Huang, W.S. Ng, J. Liu, Z. Wang, Z. Wang, H. Hu, C. Zhi, 3D spacer fabric based multifunctional triboelectric nanogenerator with great feasibility for mechanized large-scale production, *Nano Energy*. 27 (2016) 439–446. doi:10.1016/j.nanoen.2016.07.016.
- [84] H. Shirakawa, E.J. Louis, A.G. MacDiarmid, C.K. Chiang, A.J. Heeger, Synthesis of electrically conducting organic polymers: halogen derivatives of polyacetylene, (CH)_x, *J. Chem. Soc. Chem. Commun.* (1977) 578. doi:10.1039/c39770000578.
- [85] S. Cui, Y. Zheng, J. Liang, D. Wang, Conducting polymer PPy nanowire-based triboelectric nanogenerator and its application for self-powered electrochemical cathodic protection, *Chem. Sci.* 7 (2016) 6477–6483. doi:10.1039/C6SC02562E.
- [86] J. Wang, Z. Wen, Y. Zi, P. Zhou, J. Lin, H. Guo, Y. Xu, Z.L. Wang, All-Plastic-Materials Based Self-Charging Power System Composed of Triboelectric Nanogenerators and Supercapacitors, *Adv. Funct. Mater.* 26 (2016) 1070–1076. doi:10.1002/adfm.201504675.
- [87] S. Zhao, J. Li, D. Cao, G. Zhang, J. Li, K. Li, Y. Yang, W. Wang, Y. Jin, R. Sun, C.P. Wong, Recent Advancements in Flexible and Stretchable Electrodes for Electromechanical Sensors: Strategies, Materials, and Features, *ACS Appl. Mater. Interfaces*. 9 (2017) 12147–12164. doi:10.1021/acsami.6b13800.
- [88] Z. Li, G. Ma, R. Ge, F. Qin, X. Dong, W. Meng, T. Liu, J. Tong, F. Jiang, Y. Zhou, K. Li, X. Min, K. Huo, Y. Zhou, Free-standing conducting polymer films for high-performance energy devices, *Angew. Chemie - Int. Ed.* 55 (2016) 979–982. doi:10.1002/anie.201509033.
- [89] A. Šutka, M. Timusk, J. Metsik, J. Ruža, M. Knite, U. Mäeorg, PEDOT electrodes for triboelectric generator devices, *Org. Electron. Physics, Mater. Appl.* 51 (2017) 446–451. doi:10.1016/j.orgel.2017.09.052.
- [90] S. Wang, L. Lin, Z.L. Wang, Nanoscale-triboelectric-effect enabled energy conversion for sustainable powering of portable electronics, *Nano Lett.* 12 (2012) 6339–46. doi:10.1021/nl303573d.
- [91] G. Zhu, Z.H. Lin, Q. Jing, P. Bai, C. Pan, Y. Yang, Y. Zhou, Z.L. Wang, Toward large-scale energy harvesting by a nanoparticle-enhanced triboelectric nanogenerator, *Nano Lett.* 13 (2013) 847–853. doi:10.1021/nl4001053.
- [92] S. Lee, W. Ko, Y. Oh, J. Lee, G. Baek, Y. Lee, J. Sohn, S. Cha, J. Kim, J. Park, J. Hong, Triboelectric energy harvester based on wearable textile platforms employing various surface morphologies, *Nano Energy*. 12 (2015) 410–418. doi:10.1016/j.nanoen.2015.01.009.
- [93] Z. Zhang, Y. Chen, D.K. Debeli, J.S. Guo, Facile Method and Novel Dielectric Material Using a Nanoparticle-Doped Thermoplastic Elastomer Composite Fabric for Triboelectric Nanogenerator Applications, *ACS Appl. Mater. Interfaces*. 10 (2018) 13082–13091. doi:10.1021/acsami.8b02133.
- [94] F.R. Fan, L. Lin, G. Zhu, W. Wu, R. Zhang, Z.L. Wang, Transparent triboelectric nanogenerators and self-powered pressure sensors based on micropatterned plastic films, *Nano Lett.* 12 (2012) 3109–3114. doi:10.1021/nl300988z.
- [95] C.K. Jeong, K.M. Baek, S. Niu, T.W. Nam, Y.H. Hur, D.Y. Park, G.T. Hwang, M. Byun, Z.L. Wang, Y.S. Jung, K.J. Lee, Topographically-designed triboelectric nanogenerator via block copolymer self-assembly, *Nano Lett.* 14 (2014) 7031–7038. doi:10.1021/nl503402c.
- [96] X.S. Zhang, M. Di Han, R.X. Wang, F.Y. Zhu, Z.H. Li, W. Wang, H.X. Zhang, Frequency-multiplication high-output triboelectric nanogenerator for sustainably powering biomedical microsystems, *Nano Lett.* 13 (2013) 1168–1172. doi:10.1021/nl3045684.
- [97] W.B. Ko, D.S. Choi, C.H. Lee, J.Y. Yang, G.S. Yoon, J.P. Hong, Hierarchically Nanostructured 1D Conductive Bundle Yarn-Based Triboelectric Nanogenerators, *Adv. Mater.* 29 (2017) 1704434. doi:10.1002/adma.201704434.
- [98] X.S. Zhang, M. Di Han, R.X. Wang, B. Meng, F.Y. Zhu, X.M. Sun, W. Hu, W. Wang, Z.H. Li, H.X. Zhang, High-performance triboelectric nanogenerator with enhanced energy density based on single-step fluorocarbon plasma treatment, *Nano Energy*. 4 (2014) 123–131. doi:10.1016/j.nanoen.2013.12.016.
- [99] A.Y. Choi, C.J. Lee, J. Park, D. Kim, Y.T. Kim, Corrugated Textile based Triboelectric Generator for Wearable Energy Harvesting, *Sci. Rep.* 7 (2017) 45583. doi:10.1038/srep45583.
- [100] K. Dong, Y.C. Wang, J. Deng, Y. Dai, S.L. Zhang, H. Zou, B. Gu, B. Sun, Z.L. Wang, A Highly Stretchable and Washable All-Yarn-Based Self-Charging Knitting Power Textile Composed of Fiber Triboelectric Nanogenerators

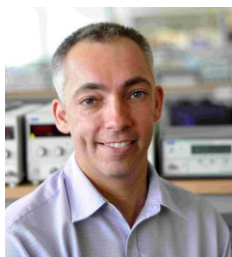
- and Supercapacitors, *ACS Nano*. 11 (2017) 9490–9499. doi:10.1021/acsnano.7b05317.
- [101] X. Li, Z.H. Lin, G. Cheng, X. Wen, Y. Liu, S. Niu, Z.L. Wang, 3D fiber-based hybrid nanogenerator for energy harvesting and as a self-powered pressure sensor, *ACS Nano*. 8 (2014) 10674–10681. doi:10.1021/nn504243j.
 - [102] J. Chen, H. Guo, X. Pu, X. Wang, Y. Xi, C. Hu, Traditional weaving craft for one-piece self-charging power textile for wearable electronics, *Nano Energy*. 50 (2018) 536–543. doi:10.1016/j.nanoen.2018.06.009.
 - [103] Y. Zi, S. Niu, J. Wang, Z. Wen, W. Tang, Z.L. Wang, Standards and figure-of-merits for quantifying the performance of triboelectric nanogenerators, *Nat. Commun*. 6 (2015) 1–8. doi:10.1038/ncomms9376.
 - [104] V. Nguyen, R. Yang, Effect of humidity and pressure on the triboelectric nanogenerator, *Nano Energy*. 2 (2013) 604–608. doi:10.1016/j.nanoen.2013.07.012.
 - [105] V. Nguyen, R. Zhu, R. Yang, Environmental effects on nanogenerators, *Nano Energy*. 14 (2014) 49–61. doi:10.1016/j.nanoen.2014.11.049.
 - [106] G. Zhu, Y.S. Zhou, P. Bai, X.S. Meng, Q. Jing, J. Chen, Z.L. Wang, A shape-adaptive thin-film-based approach for 50% high-efficiency energy generation through micro-grating sliding electrification, *Adv. Mater*. 26 (2014) 3788–3796. doi:10.1002/adma.201400021.
 - [107] F. Xi, Y. Pang, W. Li, T. Jiang, L. Zhang, T. Guo, G. Liu, C. Zhang, Z.L. Wang, Universal power management strategy for triboelectric nanogenerator, *Nano Energy*. 37 (2017) 168–176. doi:10.1016/j.nanoen.2017.05.027.
 - [108] A. Ghaffarinejad, J.Y. Hasani, R. Hinchet, Y. Lu, H. Zhang, A. Karami, D. Galayko, S.-W. Kim, P. Basset, A conditioning circuit with exponential enhancement of output energy for triboelectric nanogenerator, *Nano Energy*. 51 (2018) 173–184. doi:10.1016/j.nanoen.2018.06.034.
 - [109] Y. Song, J. Zhang, H. Guo, X. Chen, Z. Su, H. Chen, X. Cheng, H. Zhang, All-fabric-based wearable self-charging power cloth, *Appl. Phys. Lett*. 111 (2017) 073901. doi:10.1063/1.4998426.
 - [110] X. Pu, W. Hu, Z.L. Wang, Toward Wearable Self-Charging Power Systems: The Integration of Energy-Harvesting and Storage Devices, *Small*. 14 (2018) 1702817. doi:10.1002/sml.201702817.
 - [111] H. Wu, Y.A. Huang, F. Xu, Y. Duan, Z. Yin, Energy Harvesters for Wearable and Stretchable Electronics: From Flexibility to Stretchability, *Adv. Mater*. 28 (2016) 9881–9919. doi:10.1002/adma.201602251.



Watcharapong Paosangthong is a PhD student in Smart Electronic Materials and Systems Research Group at the University of Southampton, UK. He received his Diplom-Physiker Univ. degree in Physics from the Technische Universität München, Germany in 2011 and his MSc degree in MicroElectroMechanical Systems from the University of Southampton, UK, in 2017. From 2012 to 2016, he worked as research assistant and process engineer at Thai Microelectronics Center, Thailand. His research interests include triboelectric generator, energy harvesting, sensor systems, e-textiles and MEMS.



Russel Torah graduated with a BEng(hons) in Electronic Engineering and an MSc in Instrumentation and Transducers, both from the University of Southampton. In 2004 Russel obtained a PhD in Electronics from the University of Southampton. Since 2005 he has been a full-time researcher at the University of Southampton where he is currently a Senior Research Fellow. In 2011 Dr Torah co-founded Smart Fabric Inks Ltd specialising in printed smart fabrics. His research interests are currently focused on smart fabric development but he also has extensive knowledge of energy harvesting, sensors and transducers. Dr Torah has 112 publications and 1 patent.



Professor Steve P Beeby obtained his PhD from the University of Southampton, UK, in 1998 and has since been awarded two prestigious EPSRC Research Fellowships. He is currently Head of the Smart Electronic Materials and Systems research group. His research interests include energy harvesting, e-textiles, MEMS and active printed materials development. He founded the UK's Energy Harvesting Network and Chairs the International Steering Committee for the PowerMEMS conference series. He has over 250 publications and an h-Index of 46 with >12800 citations. He is a co-founder of Perpetuum Ltd, a University spin-out based upon vibration energy harvesting formed in 2004.